Submitted to Physics of Plasmas, March 27, 1996

Confinement Analysis in L-Mode of Hydrogen Isotope Experiments on TFTR

Cris W. Barnes,[*] S. D. Scott,

M. G. Bell, R. Bell, R. V. Budny, C. E. Bush,[†] E. D. Fredrickson, B. Grek,

K. W. Hill, A. Janos, J. H. Kamperschroer, P. H. LaMarche, D. K. Mansfield,

H. K. Park, C. K. Phillips, A. T. Ramsey, J. Schivell, B. C. Stratton,

E. J. Synakowski, G. Taylor, J. R. Wilson, M. C. Zarnstorff

Princeton Plasma Physics Laboratory,

Princeton, NJ 08543

PACS: 52.55.Fa

[*]Physics Division, Los Alamos National Laboratory, Los Alamos, NM 87545

[†]Oak Ridge National Laboratory

Abstract

The effect of isotope on confinement in high-recycling, L-mode plasmas is studied on the Tokamak Fusion Test Reactor (TFTR) by comparing hydrogen and deuterium plasmas with the same magnetic field and similar electron densities and heating power, with both Ohmic and deuterium-neutral-beam heating. Following a long operational period in deuterium, nominally hydrogen plasmas were created through hydrogen glow discharge and hydrogen gas puffing in Ohmic plasmas, which saturated the exposed limiter surface with hydrogen and raised the H/(H+D) ratio from 10$\pm$3% to 65$\pm$5%. Ohmic deuterium discharges obtained higher stored energy and lower loop voltage than hydrogen discharges with similar limiter conditions. Neutral-beam power scans were conducted in L-mode plasmas at minor radii of 50 and 80 cm, with plasma currents of 0.7 and 1.4 MA. To minimize transport differences from the beam deposition profile and beam heating, deuterium neutral beams were used to heat the plasmas of both isotopes. Total stored energy increased approximately 20% from nominally hydrogen plasmas to deuterium plasmas during auxiliary heating. Of this increase about half can be attributed to purely classical differences in the energy content of unthermalized beam ions. Kinetic measurements indicate a consistent but small increase in central electron temperature and total stored electron energy in deuterium relative to hydrogen plasmas, but no change in total ion stored energy. No significant differences in particle transport, momentum transport, and sawtooth behavior are observed. Overall, only a small improvement ($\sim$10%) in global energy confinement time of the thermal plasma is seen between operation in hydrogen and deuterium.

I. Introduction

Plasma confinement in tokamaks is dominated by non-collisional, "anomalous" processes driven by turbulent instabilities. Neoclassical and simple, single-species, gyro-Bohm theoretical models of plasma transport predict that lighter plasma ions, with smaller ion gyroradii, should cause less turbulent transport.[1,2] More sophisticated models which include multiple ion species and other effects can predict the reverse.[3] Experimentally, the effect of isotope on heat, particle, and momentum transport, plasma edge conditions, and sawteeth has been studied on a number of tokamaks in several plasma regimes, and with several forms of heating. Improved energy confinement in deuterium plasmas relative to hydrogen has been observed with Ohmic heating alone, as well as with neutral beam heating, ion cyclotron resonance heating, lower hybrid heating, and electron cyclotron heating. Favorable isotope scaling (improving with mass towards fusion relevant fuels of deuterium and tritium) of energy and particle transport was first observed in TFR[4] and Alcator.[5] There was subsequent experimental work on ISX-A,[6] PDX,[7] Doublet III,[8–10] Alcator-C,[11,12] T-11,[13] ASDEX,[14–27] JET,[28–31] JFT-2M,[32] TEXTOR,[33] and FT.[34] A favorable isotope effect on confinement has been realized in L-mode plasmas as well as in various improved operating regimes such as the H-mode, in the I-mode regime of TEXTOR, and in the supershot regime of TFTR. Improved confinement is commonly observed in deuterium relative to hydrogen plasmas, although the strength of the effect appears to vary considerably with the type of plasma heating and the regime of operation. The relationship of this previous work to the data of this paper from TFTR is discussed in Section III.

This paper reports transport measurements on TFTR comparing hydrogen to deuterium L-mode plasmas with identical magnetic fields and similar electron densities and heating power, with both Ohmic and deuterium-neutral-beam heating. The H/(H+D) ion particle ratio was varied from $10 \pm 3\%$ in "deuterium" discharges to $65 \pm 5\%$ in "hydrogen" discharges. Comparisons were obtained at two values of the plasma current (0.7 and 1.4 MA), and at two different aspect ratios (R/a =

2.45/0.80 [m] and 2.15/0.50 [m]). During deuterium neutral beam heating, the total stored energy and global energy confiement time is approximately 20% higher in the deuterium plasmas relative to the hydrogen plasmas. About half of this increase is attributable to classical changes in the beam stored energy from the longer beam-ion slowing down time in deuterium plasmas, indicating that the isotope effect on local confiement properties is favorable, but relatively weak. Changing the thermal isotope also causes small variations in the calculated fraction of beam power which is collisionally coupled to ions and electrons (with a greater fraction going to electrons in deuterium plasmas); this analysis is included in the local transport analysis (see Section II.B.8). For auxiliary-heated plasmas at the same current and density, the deuterium plasmas achieve a modestly higher core ($r/a \leq 0.3$) electron temperature, but no increase in central ion temperature or total ion energy content. No isotope effect on central momentum confiement is observed. In addition, no isotope effect on sawtooth behavior or plasma edge conditions (edge electron density and hydrogenic particle inflx) is seen in Ohmic plamas or during auxiliary heating.

Comparing the beam-heated plasmas at 0.7 and 1.4 MA, there appears to be little variation in the strength of the isotope effect on global confiement with plasma current, although it extends over a larger fraction of the plasma cross-section at lower current. No appreciable effect of plasma aspect ratio or minor radius on the strength of the isotope effect is discerned.

Ohmic density scans indicate some evidence of improved global energy confiement in deuterium relative to hydrogen, however the difference is less than the scatter in performance amongst nominally similar deuterium density scans. For the most comparable hydrogen and deuterium density scans, the loop voltage is lower in deuterium than in hydrogen, the Z_{eff} is higher, and the stored energy is slightly higher. The trends in Ohmic confiement for all density scans are consistent with increased plasma radiation from the core plasma decreasing power flw into the scrape-off layer, which somehow improves the confiement.

II. Experiment and Results

A. Conversion to hydrogen

The experiments with deuterium plasmas were performed fist. Prior to these experiments, TFTR had been operated without hydrogen gas injection for several years, thereby reducing the hydrogen content in the exposed surface of the carbon-carbon composite limiter. Nevertheless, the immense reservior of hydrogen buried more deeply in the limiter kept the H/(H+D) ratio at the plasma edge about 7%–15% by affecting the ratio of hydrogen to deuterium inflx from the limiter. The H/(H+D) ratio has been reduced to as low as 7% immediately after boronization using deuterium, and increased to over 90% immediately after boronization using hydrogen.[35] To convert to hydrogen, a glow discharge was performed for two hours, increasing the H/(H+D) ratio to about 50%. The near-surface of the limiter was then saturated by puffig $\sim$750 Torr liters of hydrogen gas over 11 Ohmic discharges. At the end of the saturation campaign, a moderate plasma density ($\overline{n}_e = 4.1 \times 10^{19}\ \mathrm{m}^{-3}$) was sustained solely by hydrogenic inflx from the limiter surface, and a H/(H+D) ratio of up to 70% was achieved. In an attempt to increase the hydrogenic content further, the limiter was then conditioned[36] with a series of 35 Ohmic (helium pre-fi) plasmas, then re-saturated with hydrogen gas puffig in subsequent series of three Ohmic discharges which deposited an additional 360 Torr-liters into the torus vessel. This procedure failed to increase the H/(H+D) ratio beyond the 70% achieved in the fist saturation. The transport studies of hydrogen beam-heated plasmas were started immediately after this cycle of hydrogen saturation. Additional hydrogen gas puffig was used in the beam-heated shots, with most of the inflx occuring in the Ohmic prelude before the start of beam injection. The H/(H+D) ratio dropped by a few percent each shot, presumably from deuterium injected by the beams, cold deuterium gas streaming from the beams into the torus, and migration of hydrogen and deuterium in the exposed limiter surface from plasma heating. Typically, 5–6 beam-heated discharges could be taken before the H/(H+D) ratio dropped to $\sim$60%. To maintain the maximum possible hydrogen plasma content during beam injection, the limiter was then conditioned with another cycle of Ohmic helium cleanup shots, followed by a combination of Ohmic and beam-heated shots with strong hydrogen gas puffing. Over the course of these experiments, the cycle of hydrogen-saturation and helium-cleanup was repeated four times, during which nearly 2200 Torr-liters of hydrogen gas were puffed into the vessel (the nominal capacity of the near-surface of the limiter for hydrogen gas is approximately 800–1000 Torr-liters). The maximum hydrogen content of the limiter influx remained below 70% throughout.

B. NBI L-mode comparison

1. Discharge conditions

Comparisons of hydrogen and deuterium plasmas in neutral-beam-heated discharges under high-recycling "L-mode" conditions[37,38] were obtained at identical plasma current and toroidal magnetic field, and similar density and beam power. Both large (major radius R = 2.45 m, minor radius a = 0.80 m) and small (R = 2.15 m, a = 0.50 m) plasmas were studied.[39] The current through the toroidal field coils was kept constant for all plasmas reported here, yielding a central toroidal magnetic field of 4.8 Tesla for the large plasmas and 5.5 Tesla for the smaller plasmas. For the hydrogen plasmas, the pulse length of deuterium neutral beam injection was restricted to only 0.5 seconds to minimize the dilution of the hydrogen. For these experiments, plasmas of both isotopes were heated by deuterium neutral beams. The use of hydrogen beams to heat the hydrogen plasmas would have modestly increased the achieveable H/(H+D) ratio; however, it was precluded by technical difficulties of operating the beam sources in hydrogen. In addition, using deuterium beams exclusively improved the accuracy with which intrinsic heating and confinement differences between hydrogen and deuterium plasmas could be discerned. Using the same beam isotope for plasmas of both isotopes substantially reduced differences in beam penetration and the systematic relative uncertainty in beam power that would otherwise have existed if different beam isotopes had been employed.

Deuterium beam ions do slow down more rapidly in a hydrogen thermal plasma, causing modest differences in the beam stored energy in the two cases. Since the slowing down rate, $\nu_s^{d/i'}$, of a fast ion such as a deuteron on a thermal ion i' scales with the ratio of their mass $\mu' = m_{i'}/m_d$ as

$$\nu_s^{d/i'} \propto \left(\frac{1}{2} + \frac{1}{\mu'}\right) \tag{1}$$

the ratio of beam deuterons slowing down on thermal hydrogen to slowing down on thermal deuterium is $\nu_s^{d/h}/\nu_s^{d/d} \sim 3/2$. The critical energy at which beam ions share equal collisional power with thermal ions and electrons also changes with the mass of the thermal species, with

$$\frac{E_{\text{crit}}^{D\rightarrow H}}{E_{\text{crit}}^{D\rightarrow D}} \sim 2^{2/3}. \tag{2}$$

Thus, for a fixed injection voltage, the higher critical energy for hydrogen yields relatively less beam power delivery to the electrons and more to the ions. To minimize dilution of the hydrogen target plasma by deuterium beams and the contribution of beam stored energy, the experiments were conducted at moderate density ($3.0 - 3.5 \times 10^{19}$ m^{-3}), and beam power was restricted to a maximum of 7.6 MW, corresponding to injection of only three of the available 12 beam sources on TFTR. In the deuterium plasmas, power scans with 3, 2, and 1 neutral beam sources were obtained in single discharges during a two-second beam pulse. Beam voltage was maintained at a constant 95 keV for the experiments with both isotopes. All beam power was injected tangentially in the same direction as the plasma current (co-injection) to drive measureable toroidal rotation [$v_\phi(0) < 3 \times 10^5$ m/s] to allow studies of momentum transport. Figure 1 shows time-dependent waveforms of diamagnetic stored energy, neutral beam power, line-averaged density, and central rotation velocity for both a deuterium and a hydrogen discharge with comparable density at 4.65 MW injected power.

Density scans were performed in deuterium to provide the best chance of matching data from the subsequent time-limited hydrogen operation. For both the deuterium and hydrogen discharges above an average density of $\bar{n}_e > 2.5 \times 10^{19}$ m^{-3} the Z_{eff} was quite low, between 1.2–1.5. The radial profile of Z_{eff} inferred from visiblebremstrahlung array measurements is consistent with it being flat in radius. The global confinement time compared to Goldston scaling [37] values of τ_{Aachen} ranged from 0.68–1.09 for hydrogen and 0.73–1.40 for deuterium.

2. Diagnostics

The electron, ion, and beam stored energy contents were analyzed using the one-dimensional, steady-state transport code SNAP[40,41] based on measured density and temperature profiles. The electron density profile was measured by a ten-chord Multi-channel InfraRed Interferometer[42] mapped to minor radius using a "slice & stack" algorithm.[43] Electron temperature profiles were measured by Thomson Scattering[44] and two types of Electron Cyclotron Emission (ECE): Radiometer[45] looking at first harmonic, and Michelson interferometer[46,47] looking at second harmonic. The Thomson profiles were mapped from their diagnostic grid in major radius using the same algorithm used for the electron density profile, while the ECE profiles were mapped to minor radius based on the Shafranov shift profile computed by SNAP. Visible Bremsstrahlung measurements[48] were used to infer total Z_{eff} along multiple lines of sight, and an X-ray pulse height analysis system[49] measured the Z_{eff} contribution from metal impurities in the plasma core. The H/(H+D) ratio of the hydrogenic influx from the limiter was measured by a 0.64 m Czerny-Turner visible spectrometer with a 2400 line/mm grating and a 1024 channel intensified photodiode array. The sight line of the spectrometer was radially through the plasma, and the image of the entrance slit fell on the midplane of the limiter with a 30 cm high by 0.5 cm wide footprint. These H/(H+D) ratios measured at the edge are assumed to remain constant across the entire minor radius, consistent with the strong dominance of wall hydrogenic influx to beam fuelling in the high-recycling L-mode regime. Edge hydrogenic-neutral influx was inferred[50] from measurements of an array of five H_α detectors[48] viewing the bumper limiter.

The ion temperature and toroidal rotation velocity were measured with 8 cm spatial resolution at ten locations in the plasma by CHarge Exchange Recombination Spectroscopy[51] (CHERS). Since there are larger uncertainties in the CHERS measurements inside the major radius arising from beam attenuation and poorer signal-to-noise ratios, only data points from the portion of the CHERS profiles on the outboard-side of the magnetic axis were mapped to minor radius. Diagnostic assess restrictions limited the CHERS measurements to just four radial locations for the smaller (R = 2.15 m) discharges. To analyze the Doppler shift of the measurement, the toroidal rotation velocity was assumed to have zero velocity at the edge of the plasma at the very beginning of the neutral beam injection in each shot. Effects of "ion plumes" on the CHERS measurement[52] is expected to be very small and, more importantly, to not differ between deuterium and hydrogen plasmas.

3. Variations in Electron Temperature Diagnostics

Profiles from all three electron temperature diagnostics have been compared at different phases of sawteeth. While the central temperature during the period of the sawteeth varies by up to 15%, the total electron stored energy only varies by up to 5% and generally only by 2%. The analysis of total stored electron energy reported below, and all subsequent analysis, uses data time-averaged over entire sawteeth period excluding the instant of the crash. This removes the effects of comparing radiometer, with its fast time resolution, to Michelson, which acquires a pair of radial profiles every 22 msec. The radiometer suffered from mode switching in the backward wave oscillator of its first (low frequency, outboard) band during the hydrogen operation, so the inboard part of the profile was used in all the analysis.

Figure 2 shows the electron stored energy inferred from each of the three diagnostics as a function of total input power for the large plasmas. The radiometer measurement of electron temperature profile consistently yields 10–15% more stored energy than the Michelson profile, with the Thomson profile perhaps equal or slightly greater than radiometer. Analysis based solely on the radiometer $T_e(R)$ profile measurement shows a clear increase in electron stored energy (30%) between hydrogen and deuterium plasmas at the same total input power. Comparable analysis based solely on the Michelson shows a smaller increase of approximately 15%. Because the Thomson scattering data was taken usually during the Ohmic phase during the deuterium experiments to obtain impurity information from x-ray pulse-height analysis, there are insufficient pairs of data from Thomson to reach a conclusion. While the difference in total stored electron energy content between hydrogen and deuterium operation is only comparable to the discrepancy among the different electron temperature diagnostics, we believe there is a 20% $\pm$ 8% difference in the electron stored energy between the deuterium and hydrogen L-modedischarges. This result is not necessarily inconsistent with an isotope effect on electron energy content as large as the square-root of the mass ratio ($\tau_{Ee} \propto \langle A \rangle^{1/2}$) since there was only a 50% change in the H/(H+D) ratio. (The average mass A changed from 1.35 ± 0.05 in hydrogen to 1.90 ± 0.03 in deuterium in these experiments.) The estimated uncertainty is dominated by the differences between the absolute calibration of the two ECE diagnostics. The change in electron stored energy is consistent with similarly small changes in stored energy seen in L-mode discharges on other devices. For the remaining confinement and transport analysis in this paper the data from the Michelson interferomenter will be used, based on its relative precision, lack of noise problems, and availability for nearly all discharges.

4. Kinetic analysis model

Beam deposition is determined in SNAP by computing the attenuation of incident beam neutrals along their linear trajectory through the plasma, including ionization and charge-exchange processes. The beam-ion distribution function, the local beam power delivery to ions and electrons, and the beam-ion loss rate to charge-exchange are calculated from a solution of the Fokker-Planck equation in the rotating plasma frame, using classical models of deposition[53] and slowing down[54] confirmed by experiment. Partial recapture of the beam charge-exchange neutral flux is modelled approximately by assuming that a fixed fraction (65%) of such neutrals is recaptured locally. The fraction was chosen by comparison with more detailed TRANSP[55] simulations of similar discharges. The radial profile of neutrals is computed in SNAP by a generalization of the ANTIC code[56] to handle multiple species. Details of these calculations are discussed in Ref. 40. The Ohmic heating power to the plasma is calculated assuming resistive equilibrium using neoclassical resistivity,[57] including beam-driven and bootstrap-current[58] contributions.

5. Global energy confinement

Figure 3 plots the total thermal electron energy, total thermal ion energy, and total plasma energy (as measured by a diamagnetic loop) as a function of heating power for all discharges in the experiment. The trends exhibit typical L-mode behavior: the incremental confiement time (the slope of the data) increases somewhat with plasma current and varies weakly, if at all, with plasma density. The largest effect is on the "Ohmic energy offset" (the y-intercept of a linear fi) which increases proportional to plasma current. The hydrogen energy confiement time is about 20% less than the deuterium confiement time, with most of the difference in the stored energy observed in the electrons and none in the ions. The variability in stored energy at similar heating power for the data points in Fig. 3 is caused by variation in the line-integrated density during the experiment; as the density increases the beam stored energy decreases dramatically, as do the electron and ion stored energies, while the beam charge-exchange losses increase and hence the total input power decreases.

Typically half of the total stored energy increase between hydrogen and deuterium discharges is from more beam stored energy arising from the longer slowing down time in deuterium at the same electron density [Eqn. (1)]. The incremental confiement time changes hardly at all with isotope; it appears to be the "Ohmic offset" that increases with deuterium.

With the different beam timings used with the hydrogen and deuterium discharges (see Fig. 1), the plasmas inductance ℓ_i is 2%–8% different at the times of comparison (generally higher in hydrogen because of later beam injection). Because of the observed correlation of ℓ_i and confiement[59] with $\partial(\tau_E/\tau_{\text{L-mode}})/\partial\ell_i \sim 0.5$ there might be an additional few percent difference in confiement hidden by our experimental method.

6. Uncertainty analysis

The error bars used in this paper on the diagnostic measurements are "relative" uncertainties that represent the uncertainty in comparing measurements from deuterium discharges to those from hydrogen discharges (of similar magnetic field and density). The error bars shown exclude additional, systematic uncertainties common to measurements from both plasmas. For the CHERS data the uncertainties are dominated by background subtraction and photon statistics, which worsen towards smaller major radius. For the second harmonic electron cyclotron emission (ECE) (see below) the relative uncertainty is estimated at $\pm$3% when the magnetic field is kept the same. The total relative uncertainty on the injected beam power, for the ion sources chosen for this experiment, is 3%.[60]

Comparisons of the total stored energy and neutron emission calculated by the SNAP code, based on the kinetic measurements of density and temperature, with direct diagnostic measurements of the same quantities provide independent cross-checks of the diagnostic measurements. For these plasmas the calculated stored energy and neutron emission agree relatively well with measurements, validating both the neutral beam calculations used in the transport analysis and assumptions about the central H/(H+D) ratio. As shown in Figure 4, the diamagnetic measurement appears consistently 65 kJ low; this diagnostic effect is within the measurement absolute error. The calculated neutron source strength is consistently only about 85% of the measurement; this is the same result as found in previous analysis of co-injected discharges on TFTR.[61,62] This discrepancy in co-injected discharges is not explainable by decreased neutrals from recycling, increased charge exchange re-capture, decreased hydrogen content in deuterium discharges, or decreased Z_{eff} in the center of the plasma, although all these factors working together might explain the difference. Adjusting the measured magnetic stored energy by the 65 kJ, the SNAP analysis agrees with the measurement within $\pm$5% (one-sigma). The SNAP calculations are within $\pm$10% (one-sigma) of the 85% average of the neutron measurements. Both results are in very good agreement within the remaining relative uncertainties of the diagnostics. Our presumption that 0.5-second beam injection would not dilute the hydrogen significantly appears correct, both because of spectroscopic measurement of the H/(H+D) ratio (weighted to the edge region) and because of the agreement of the neutron source strength calculation with its measurement (weighted to the central core).

7. Particle confinement

The neutral density profile calculated by SNAP requires as a boundary condition the incident flux of hydrogenic neutrals at the plasma edge. This flux is inferred from measurements of H_α light along five sightlines viewing the inner bumper limiter at different poloidal angles. Based on comparisons of the poloidal distribution of H_α light to numerical simulations of the neutral density in the plasma and scrape-off region by the DEGAS,[50] the hydrogenic influx is modelled to be proportional to the total observed H_α light.[63,64] Consistent with DEGAS simulations, the constant of proportionality is assumed to be the same for hydrogen and deuterium plasmas. The resulting electron particle sources are shown in Figure 5, illustrating no significant difference between the hydrogen (pluses) and deuterium (x's) discharges.

Both the magnitude of the recycling light and its poloidal distribution are nearly identical for comparable hydrogen and deuterium discharges of matched size, field, and density. Since the beam fueling and density profile shapes are the same, we conclude there is no significant change in particle confinement between our hydrogen and deuterium discharges, in contrast to observations in JET.[31] The inferred global electron particle confinement times are 10–50 milliseconds.

8. Profile comparison and power-balance analysis

Figure 6 shows profile data during neutral-beam injection from deuterium and hydrogen discharges with similar density profiles. Very similar density-profile pairs were obtained for the large minor-radius plasmas (a = 0.80 m) at 1.4 MA [Fig.6(a–c)]. The electron temperature was consistently lower in hydrogen (by $\sim$10–30%) in the center ($r/a \leq 0.3$) of the discharge, but nearly identical outside that radius. The ion temperature showed no consistent variation. Because the discharges are at the same electron density and nearly the same electron temperature with the same neutral beam injection, relative differences from corrections caused by ion plumes on the CHERS measurements of the central ion temperature are expected to be very small. At the lower current of 0.7 MA [Fig. 6(d–e)] the density pairing is not as good; using the comparisons as is, the electron temperature difference may now extend over most of the plasma radius, *i.e.* there may be a bigger isotope effect at low current. There is also a hint of a slight systematic change in the ion temperature at low current. For the small plasmas at 0.7 MA [Fig.6(f–g)] there exist only 4 radial locations of ion temperature measurement, which do not extend to the plasma center. The electron temperature is higher in the deuterium discharges, again apparently over most of the plasma radius. In most cases a deuterium discharge can be found with electron density just on the other side of the hydrogen data; even in these cases, a difference in electron temperature remains, consistent with results observed on ASDEX.[19,21,22,24] Table 1 lists a comparison of plasma parameters in these shots paired by density.

The power balance in these hydrogen and deuterium discharges are relatively similar to each other and are typical of TFTR L-mode discharges. One example typical of the transport analysis is shown in Figure 7 for the deuterium plasma of the pair of discharges at 1.4 MA, 2.45 m radius and 4.65 MW of NBI. For these high-recycling discharges with constant gas feed to maintain high density, the effects of neutrals are very severe in the outer 12% of the plasma (beyond r = 0.7 m).[63] This region is ignored for the local transport analysis because of uncertainties in charge exchange loss and convective power flow. Of the 4.70 (4.62) MW of neutral beam injection in the deuterium (hydrogen) discharge, there was only 0.01 (0.05) MW of shine-through or orbit-loss power, but 0.98 (0.96) MW of beam charge-exchange loss. Including 0.54 (0.59) MW of Ohmic power there was 4.25 (4.20) MW of total heating power into the plasma. Total beam power delivered to ions was 1.98 (2.04) MW and total power delivered to electrons was 1.46 (1.21) MW.

To assess changes in the power balance, it is convenient to compare the power fluxes integrated out to a given radius normalized by the total heating power inside the same radius. For the electrons, the Ohmic input power is 25%–15% of the total and the beam heating is 18%–38% for a total of 43%–53% (the quoted range is across the profile from the center to the edge). 3%–12% of this is radiated; -3%–8% is coupled to the ions; and 11%–20% is calculated to be convected (transported by the calculated particle flux). The remaining 52%–62% that goes to the ions is almost all beam heating to ions plus thermalization energy, with $< 3\%$ input power from viscous damping near the edge. The ion convective losses range from 11%–22% inside $r = 0.7$ m; hence these plasmas are ion conduction dominated as is typical of TFTR L-mode discharges.

As expected, there are small differences in the heating to the electrons or ions even for exactly the same deuterium beam injection into a hydrogen or deuterium discharge. As with Ohmic discharges (see below) the loop voltage and hence the Ohmic input power to the electrons is lower in deuterium discharges than in hydrogen. Differences in the beam-ion thermalization rate [Eqs. (1) and (2)] cause the relative beam heating to electrons to be greater in deuterium plasmas and hence the total heating power to the electrons to be slightly greater in deuterium than hydrogen. Thus, at least part of the observed increase in electron temperature in deuterium can possibly be explained by increased heat input, without requiring or implying any intrinsic improvement in confinement. The difference in the conducted or conducted-plus-convective power flows is comparable in magnitude to the uncertainty in the electron-ion coupling terms. Slightly less power is deposited by the beams on the ions in deuterium as well as less viscous damping because of slower rotation. Thus, despite little observed improvement in temperature and energy of the ions in deuterium there may actually be an intrinsic confinement improvement in the ion channel.

To assess whether the observed temperature increases in deuterium plasmas reflect primarily differences in heating versus differences in intrinsic confinement, the calculated power and momentum flows can be divided by the measured gradients to determine diffusivities. Because of the large uncertainties in the convected power (albeit not necessarily *relative* uncertainty in this case) the total effective thermal diffusivity is presented, where $\chi_{j_{\rm tot}}$ is defined from the total conducted plus convected power flux $\boldsymbol{Q}_j$ as

$$\boldsymbol{Q}_j = \chi_{j_{\rm tot}} \boldsymbol{n}_j \boldsymbol{k}_B \nabla \boldsymbol{T}_j \tag{3}$$

for species $\boldsymbol{j}$. Figure 8 shows the total effective diffusivities, and the momentum diffusion coefficients, for the hydrogen and deuterium discharges of Fig. 7. The error bars shown on these plots are the relative uncertainty in the analysis between the hydrogen and deuterium discharges. They are estimated from using the relative uncertainty for each diagnostic input and running an ensemble of 36 SNAP runs with the inputs varied randomly according to their individual uncertainties.[38] There is no significant change in thermal transport except for the electrons inside 0.25 m minor radius. The improved confinement of the electrons is consistent at all powers. Figure 9 shows the integrated confinement time at the one-quarter minor radius for both electrons and ions for the three powers with matched density for the large 1.4 MA discharges. The electron confinement shows an improvement from hydrogen to deuterium at all powers and the ion confinement shows none.

9. Isotope effect on sawteeth

An attempt to compare the effects of sawteeth[15,21,22,31] was made by comparing the paired discharges having the same neutral beam power and electron density profile. At 2.45 m major radius with the all-co injection, sawteeth were “stabilized” in both isotopes for the duration of the neutral beam pulse at 4.6 MW and above for 0.7 MA, and at 6.8 MW and above for 1.4 MA discharges. (These are not accurate threshold levels, but represent which discharges in this experiment had no sawteeth.) The sawtooth period was the same in hydrogen and deuterium for the 2.5 MW, 1.4 MA, 2.45 m discharges and for the 4.6 MW, 0.7 MA, 2.15 m discharges. This result differs from the effect of isotope on sawteeth observed in ASDEX[21,22,24,27] and JET.[31] Only one long sawtooth was seen at 4.7 MW in the 1.4 MA, 2.45 m discharges, and hence the period cannot be accurately compared. The magnitude of the sawteeth (if any) was too small to measure in the 2.15 m, 2.2 MW discharges.

The central electron temperature rise or “re-heat rate” was the same within 10% uncertainty for the 2.45 m plasmas, consistent with the input power to the electrons being approximately the same for the hydrogen and deuterium cases. However, the electron temperature re-heat was 70% faster in deuterium (despite the same sawtooth period) in the 2.15 m plasmas, even though again the calculated input power to the electrons was in this case *less* in the deuterium case.

10. Isotope effect on momentum transport

ASDEX reports “a well-developed isotope effect”[26] in momentum transport. However, on TFTR in L-mode discharges there is no difference in the momentum confinement between deuterium and hydrogen. Figure 10 shows nearly proportional increase in central momentum with applied torque, but with no observable difference between deuterium and hydrogen. That is, the hydrogen discharges actually rotate nearly 50% *faster* than deuterium discharges (see Fig. 1), which is just the difference in the H/(H+D) ratio. The effect is not just in the center; as seen in a typical case Fig. 8 there is no significant difference in the momentum diffusivity at any radii.

C. Ohmic comparison

During the initial hydrogen gas-up and clean-up a 50-shot density scan was obtained, with H/(H+D) varying between 50–70%. The behavior of global energy confinement time in this scan can be compared to that obtained in a number of Ohmic density scans in deuterium plasmas of the same size, current, and toroidal field. Overall, the small difference in τ_E between the hydrogen and deuterium plasmas is less than the variation amongst the various deuterium scans themeselves. If we restrict attention to those scans having the most similar edge conditions, there does appear to be an observable, favorable isotope effect on Ohmic energy confinement. Quantifying this difference requires a careful assessment of the effects of edge conditions on Ohmic plasmas.

Data from deuterium density scans were obtained from 10 TFTR experiments during 1989 and 1990. All comparisons were made for 1.4 MA, -55.7 kA TF, 2.45 m major radius discharges. Most (but not all) were conditioning discharges using helium pre-fill only. Despite the helium pre-fill used to create some of these discharges, the ion density is primarily hydrogenic species (and impurities) from the limiter. Ohmic discharges in TFTR continue to evolve resistively with seconds-long time scales, so comparisons are made near the very end of the plasma current flattop.

We can first compare the hydrogen density scan to all the deuterium scans that were obtained (see Figs. 11 and 12). The $\ell_i/2$ (representing the current density profile), the loop voltage, visible bremsstrahlung, H_α and CII recycling light, radiated power fraction, density peakedness, and stored energy have been examined. We could not compare neutron rates (and hence central ion temperature) in the Ohmic equilibrium of most of these discharges because of neutron background from the calorimeters during neutral beam conditioning. Over this extended operating period, the electron temperature diagnostics had significant systematic uncertainties (up to 15%) that precludes an evaluation of isotope effect on electron temperature in these scans. Compared to the average of the deuterium scans, the hydrogen scan has: the same $\ell_i/2$; the same loop voltage at low density, higher loop voltage (5%) at high density; slightly lower Z_{eff}; a somewhat lower radiated power fraction (40% instead of the typical 50% at all densities); the same density peakedness as a function of density[65]; about the same total stored energy at low density, but less stored energy (10 ± 5)% at high density. These trends imply that the same global confinement time at low density, *i.e.* in the linear regime. The higher voltage and lower stored energy suggests lower global τ_E in the hydrogen scan, by (10 ± 5)%, in the high density (saturated) regime. Unfortunately, the wide variation amongst the individual deuterium scans, which presumably results from differing edge conditions, makes it difficult to assert that the difference between the hydrogen scan and the average of the deuterium scans is an intrinsic isotope effect.

To minimize potential differences in energy confinement arising from variability in edge conditions, it is appropriate to focus attention on those deuterium density scans with similar gas puffing and limiter preparation to the hydrogen density scan. For one example, see the closed triangles in Figure 10 of Ref. 66. Compared to these discharges, the hydrogen loop voltage is higher while the visible bremsstrahlung signal is lower at a given density, while the electron temperatures appear close to the same, as do the total stored energies. Thus the confinement time is a little less. Time dependent measurements from specific discharges with the same line-averaged density can be compared from just these similar experiments (Fig. 13). In general the hydrogen discharges have higher loop voltage and more Ohmic heating but less diamagnetic stored energy, implying smaller global τ_E. The hydrogen discharge has the lowest confinement time, even though it is neither the highest loop voltage or lowest stored energy. This is consistent with the results documented for ASDEX[19,21] and TEXTOR,[33] including the reduction in radiated power fraction in hydrogen. A slightly lower Z_{eff} in hydrogen compared to Ohmic deuterium plasmas is "in agreement with previous experience"[21] on ASDEX, but not for their carbonized wall conditions of that paper; however, it is in agreement for the carbonized conditions reported later[24] and for the experience on TEXTOR[33]; further however, there is a 0.0 regression exponent on Z_{eff} in the confinement time in the carbonized data of Ref. 25.

Also, we observe that the hydrogen Ohmic discharges have the same sawtooth frequency (29 $\pm$ 1 sawteeth in one second) at the same density as the deuterium discharges, as opposed to ASDEX[21,24] Finally, the density peakedness, $n_{eo}/\langle n_e \rangle$, as a function of line-average density is the same on TFTR for hydrogen and deuterium, as is the ratio of edge density to line-average density, whereas a difference was again seen on ASDEX.[20,67]

The most complete study of the isotope effect on confinement and its source has been performed on ASDEX[68,19–21,23,24,27] which identified the possible strong role of edge density and density profiles. In neutral-beam-heated results we see the same amount of recycling light at a given density[63] and plasma current for both hydrogen and deuterium, within the $\sim$ 20% variation observed in deuterium discharges alone (see Fig. 5). Looking at the edge $n_e\ell$ channels for the Figure 13 plasmas shows a less than 10% difference in Ohmic discharges, with the H_α light again varying most widely between deuterium scans. Thus no discernible difference in the density at the last closed flux surface[21–24] is seen in these high-density, limiter discharges, consistent with the trend seen in auxiliary heated discharges in ASDEX.[22,24] Also, the n_e profiles in the auxiliary heated discharges of Figure 6 show the same edge values. The Ohmic density scans maintain the same density peakedness as a function of density for both hydrogen and deuterium [see Fig. 11(c)]. This is contrary to what was reported on ASDEX[68,20,24,67] and TEXTOR,[33] but the observation of an isotope dependence of the confinement with the same density profile in Ohmic discharges is consistent with later results.[21] We do see higher $P_{\rm OH}$ and lower $P_{\rm RAD}$ in hydrogen than in deuterium, and thus a higher expected power into the scrape-off layer for hydrogen even for the same particle confinement (same recycling light at the same density).

We take this opportunity to comment about some of the other deuterium scans. Deuterium discharges after boronization had significantly reduced H_α and CII light, increased confinement, but with higher radiated power and lower T_e. The deuterium confinement was best in a post-major-disruption clean-up sequence which was also the closest sequence in time to the hydrogen experiments. These deuterium discharges also had significantly less H_α recycling light, a higher radiated power fraction, low loop voltage, and high stored energy. These results are consistent with the ASDEX hypothesis that increased radiation from the Ohmic plasma reduces power flow into the scrape-off layer and reduces the scrape-off density, which somehow allows improved confinement in the core plasma. We see no significant change in density peakedness for a given total density in any of these density scans, so it does not appear that changing the density scale length is the cause of the changing global confinement.

D. ICRF

An attempt was made to compare ^{3}He minority heating by ICRF in similar deuterium and hydrogen majority plasmas. Good discharges were obtained in the deuterium plasmas, which had H/(H+D) $<$ 15%. However, in the hydrogen plasmas with H/(H+D) $<$ 70% the large deuterium fraction prevented adequate coupling of the RF power, and no comparison of the confiement could be made.

III. Disussion

To place the TFTR results in context, we provide a discussion of prior work on L-mode (and Ohmic) confiement in hydrogen and deuterium plasmas. This is not intended as a review (for example, see Ref. 27) but rather as a guide for comparison of these results.

A. Overview of Previous Experiments

The isotopic dependence of energy confiement in L-mode plasmas has been studied in Doublet-III, DIII-D, JET, ASDEX, and TFTR. On Doublet-III[9] the global energy confiement was compared during hydrogen versus deuterium beam injection into deuterium L-mode plasmas at constant beam voltage. Although there was enough scatter in the data to allow τ_E in the best-performing hydrogen discharges to overlap the poorest-performing deuterium discharges, D^o injection generally yielded higher confiement times, by 25–40%, compared to H^o injection. A strong isotope effect on confiement in DIII-D H-mode plasmas was observed, [69] with τ_E/I_p in deuterium twice the value in hydrogen.[70,71] However, the L-mode energy confiement was reported to be independent of ion species.[70] JFT-2M also found that gross energy confiement time in L-mode plasmas did not vary with gas species [32] using H^o injection into both hydrogen and deuterium. Similarly, ASDEX observed that the ratio of τ_E^*/I_p increased by a factor of 1.5 in H-mode plasmas but only by a factor of 1.2 in L-mode plasmas between hydrogen and deuterium.[15] Regression analysis of their global energy confinement data [22] yielded $\tau_E \propto \langle A\rangle^{0.27\pm0.08}$ and $\tau_E \propto \langle A\rangle^{0.57\pm0.07}$. ASDEX saw a strong isotope effect in Ohmic plasmas[68]; they normalize their auxiliary-heated confinement to remove this effect.[18] The change in heating efficiency with species mix (n_H/n_e) was studied with second harmonic hydrogen heating and a reduction found with increased hydrogen.[18] ASDEX observed weaker isotope scaling of global τ_E in beam-heated L-mode plasmas[22,27] than in the Ohmic regime, but it was still a statistically robust and reproducible effect.

The most similar work to this TFTR experiment has been done at JET. Early indications of a weakly favorable isotope effect on energy confinement in L-mode plasmas[29] were substantiated by detailed comparisons of hydrogen, deuterium, and ^{3}He plasmas with carefully matched conditions.[31] These experiments were carried out at R = 3.1 m, a = 1.1 m, κ = 1.45, I_p = 3.1 MA, B_t = 2.9 Tesla, $P_b \approx$ 6 MW, and volume-averaged electron density in the range $\langle n_e\rangle \approx (1.5 - 3.5) \times 10^{19}\mathrm{m}^{-3}$. With the exception of higher plasma current, these conditions do not differ significantly from the TFTR results reported in this paper. To maximize the difference in isotopic content, the experiments compared $H^o \rightarrow H^+$ to $D^o \rightarrow D^+$ NBI heating, while the beam voltage was adjusted (140 keV for H^o versus 100 keV for D^o) to provide similar heating profiles and similar ratios of beam power deposition to thermal ions and electrons. A deuterium contamination of the hydrogen plasmas of less than 10% was achieved. Very similar impurity content, radiated power, and radial profiles of electron density were obtained in the hydrogen and deuterium plasmas. A systematically higher global τ_E was observed in deuterium relative to hydrogen plasmas ($\Delta\tau_E \leq$ 25%), along with higher central electron temperatures. Part of this difference could be attributed to the larger beam stored energy in the deuterium plasmas, and the inferred improvement in τ_E^{th} was only about 15%.

Two-fluid analysis of the JET deuterium plasmas using measured $T_i(R)$ profiles revealed the usual L-mode behavior, that power loss through the ions was at least as important as through the electrons. The only significant limitation of these results was the lack of ion temperature profile measurements for the hydrogen discharges, which necessitated the use of single-fluid analysis assuming $T_i = T_e$ everywhere

— as had been observed, within 10%, in the deuterium plasmas. The single-fluid diffusivity χ_{eff} was only marginally lower in deuterium plasmas than in hydrogen plasmas at $r/a = 0.6$ and virtually indistinguishable at $r/a = 0.8$. The most significant isotopic effects were improved particle confinement and a longer sawtooth period in deuterium plasmas, which also had some, albeit weak, effects on τ_E and τ_E^{th}. Some of the $\sim$15% improvement in τ_E^{th} might be attributable to these effects, and the authors conclude that their data suggests, but does not prove, an isotope effect on local heat transport.

Thus, the magnitude of the isotope effect on confinement has varied among tokamaks and among operating modes within an individual tokamak. Tables 2 and 3 summarize the comparison of TFTR L-mode and Ohmic confinement scaling reported here to previously published experiements.

B. Theoretical Interpretations

There have been theoretical attempts to explain the "isotope effect". Samm *et al.* of TEXTOR[33] suggested that the transport might scale with the ion thermal velocity as if there were a fixed characteristic radial step width of stochastic magnetic field lines. Coppi[3] has hypothesized that impurity-driven modes in the edge of the plasma which create and regulate a transport barrier can explain an isotope effect. Changing the isotope of the primary ion species from hydrogen to deuterium can stabilize the mode and improve the confinement. For plasmas of the same density, current, size, and heating power he predicts a scaling in L-mode of the confinement time as $(A/\alpha_T^2)^{2/5}$. Dominguez[72] similarly derives how the presence of impurities can help stabilize the ion temperature gradient mode (however, presumably in the core of the plasma) with differing effects from different primary isotopes. He predicts in saturated, high density Ohmic conditions an $A^{0.56}/Z_i$ scaling of the confinement time. This result should also hold for L-mode discharges of similar Z_{eff} and density profiles. Scott [73] proposes that collisional electron drift waves in the edge plasma have drive terms (in "standard" notation)

$$\propto \frac{\omega_* \nu_e L_s^2}{k_0^2 V_e^2 \rho_s^2}$$

which only depends on the ion mass in the ρ_s term in the denominator. Hence in deuterium plasmas the edge transport driven by collisional electron drift waves is expected to reduce. Also, higher temperatures also reduce this drive term.

C. Comparisons of analysis

Which plasma species is the root of the isotope effect has been a source of study. The realization of favorable isotope scaling of global τ_E in low-density plasmas using Ohmic and ECH heating is strong evidence that the average ion mass affects electron heat transport. In these regimes the input power is deposited entirely to electrons, and at such low density there is little ion-electron coupling so the electrons also transport most of the radial heat flx. For example, ASDEX concluded that "the superior confiement properties of a deuterium plasma ... again seem to be a consequence of the electron transport since electron heat losses are dominating the energy balance in these discharges."[15] In Ohmically-heated pellet-fuelled ASDEX discharges it was concluded that core ion energy confiement must be close to neoclassical, since even the assumption of $\chi_i = \chi_i^{neo}$ left little energy to be conducted radially by electrons.[68] By assuming that neoclassical ion heat transport also prevailed in the outer half of the plasma,the observed isotope dependence was inferred to arise from a decrease in the electron thermal diffusivity. Similarly, ASDEX observed a favorable isotope effect even at low q_a near the density limit, where the dominance of ion heat transport was expected to be strongest,[21] consistent with previous Ohmic density scans.[6,19] In L-mode discharges on JET similar to those studied here[31] a clear increase in central electron temperature was seen; however, $T_i = T_e$ in both isotopes at all radii and no separation of power flws was done.

Most previous isotope-scaling analyses were based exclusively on the global energy confiement time measured by magnetic diagnostics, which necessarily summed together the thermal plasma energy and energy in the unthermalized beam-ion population.[14,15,17,71,70] Nevertheless, these studies were able to conclude that isotope scaling of global τ_E implied differences in transport properties of the *thermal* plasma because the beam ions were calculated to represent only a small fraction of the total stored energy. For example, the contribution of fast ions to the total stored energy was calculated to be 10-15% of the total for typical Doublet III discharges.[9] Similarly, ASDEX concluded that in comparisons of hydrogen and deuterium target plasmas both heated with hydrogen beams, the increased diamagnetism in the deuterium plasmas was too large to be explained by the larger beam stored energy in deuterium plasmas.[14,15,17,71,70] In larger tokamaks, for which the beam-ion thermalization time is longer, the fraction of total stored energy carried by the beam ions tends to be higher, and so it becomes essential to carry out a proper kinetic analysis. The analysis of JET L-mode discharges[31] summarized earlier did correct for the differing fast ion populations, and on this basis concluded that there was possibly a modest decrease in the conducted heat transport in deuterium plasmas. Local transport comparison of hydrogen and deuterium discharges has also previously been carried out for Ohmic discharges[68,22] but without direct measurement of the ion temperature profile.

Another potential confounding factor in beam-heated isotope scaling experiments is differences in the heating profile. Often global comparisons were made between D^o beams and H^o beams at the same energy. Under such conditions there is more full-energy component available in the deuterium beams, with concomitant effects on beam deposition and heating profiles. [9] For example, Doublet III concluded that "differences in the power deposition ... [could have been] partially responsible for the confinement improvement" of 25% to 40% in global τ_E observed in limiter and diverted plasmas.[9] The analysis of Doublet III energy confinement by the JAERI Team[10] also found a 30% improvement in τ_E with D^o injection over H^o injection, with 20% more power deposited on thermal ions; however, the additional effect of the differences in the heating deposition profile was not considered. JET[31] used significantly different energy beams in hydrogen (100 keV) and deuterium (140 keV) to achieve more similar power deposition profiles and fast ion effects.

The particle confinement time has also been studied comparing hydrogen and deuterium discharges. Both impurity transport[11,12] and global hydrogen particle transport[13,16,23,24,33,74,31] are more rapid in hydrogen discharges than in deuterium. However, no dependence on the ion mass was detected in hydrogen test particle transport experiments on TCA.[75]

D. Discussion of TFTR Results

The confinement analysis of these TFTR L-mode discharges differs from prior work in three important ways: 1) Only partial conversion to hydrogen from deuterium was achieved; however, this should only reduce any "isotope effect" and not remove it. 2) Deuterium neutral beam injection was used to heat the plasmas of both isotopes to reduce the effects on transport from different deposition and heating by the beams. 3) "Paired discharges" of nearly identical density profiles are analyzed to remove the important effects of differing density gradient scale length. In addition, careful attention is paid to the "relative" uncertainties in the diagnostics between the hydrogen and deuterium discharges rather than the usual "absolute" uncertainties.

The result of this analysis is that deuterium L-mode discharges in TFTR appear to have slightly better energy confinement than hydrogen discharges. The confinement appears to primarily increase in the core electrons in going from hydrogen thermal plasmas to deuterium plasmas. We see no difference in the ion stored energy, though there is a small classical reduction in ion heating. Some of the difference in the electron stored energy (seen especially in the central electron temperature) is caused by the increased power flow to the electrons in thermal deuterium discharges. Unfortunate absolute discrepancies between the different electron temperature diagnostics on TFTR makes the absolute magnitude of the "isotope effect" on the electrons uncertain. When extrapolated to comparing pure deuterium to pure hydrogen, the "isotope effect" on the total stored energy (including fast ions) could be as much as the square root of the isotopic mass; however, half of the total stored energy effect comes from classical differences in the beam stored energy. The increase in the electron *thermal* stored energy, when extrapolated to full isotopic conversion, is (20% $\pm$ 8%) (one sigma uncertainty). This corresponds to an improvement in thermal confinement proportional to $A^{0.26\pm0.11}$.

These L-mode discharges have both similarities to those studied before on TFTR and differences from those from other devices. As is typical of TFTR L-mode discharges the power balance of these plasmas is dominated by ion conduction. Convected power (energy carried by particle transport) is very important in the outer 12% of the plasma. We see, at the same density and current, nearly the same density and the same distribution and amount of H_α light from the edge of both hydrogen and deuterium discharges; hence, unlike nearly all previous experiments,[13,21–23,31] we infer nearly the *same* edge conditions and particle confinement time for plasmas of both isotopes. However, our results are consistent with the ASDEX hypothesis that increased radiation from the plasma reduces power flow into the scrape-off layer which somehow causes better overall confinement.

Using our comparisons between discharges of the same density and density profile, we see results different from previous published work on other devices. Using unbalanced (all "co-injection") neutral beam injection, we see no difference in the momentum confinement between isotopes, unlike ASDEX. [26] Despite the differing central electron temperature, TFTR also has little or no difference in sawteeth period or re-heat, again contrary to all previous experience.[15,21,22,31] At low current the improved electron confinement may extend over the entire radial profile, but it remains largest in the core. The difference in current seems more striking than any difference in plasma size or aspect ratio. Because the isotope effect is observed in TFTR discharges with very similar density profiles, it is clear that the improved deuterium confinement is not caused by any changes in the density profile.

One significant difference in our results is measurements of the toroidal rotation speed compared to ASDEX.[26] In that work the authors performed a database study of beam-heated hydrogen and deuterium L-mode plasmas. They found that the central velocity scaled with input torque L, density and plasma current as $v_o \propto (L/\overline{n}_e)^{0.61} I_p^{0.3}$ with no significant dependence on the plasma mass. This scaling implies a very strong isotope scaling of τ_ϕ since the deuterium plasmas were heavier. From profile analysis the authors inferred a scaling of radially-averaged $\chi_\phi \propto A^{-0.8}$ and a scaling of global momentum confinement time $\tau_\phi \propto A^{1.0}$. Although the statistical inference of improved momentum confinement in deuterium plasmas was clearly established, this conclusion was not substantiated by direct comparisons of momentum transport in comparably-prepared hydrogen and deuterium discharges. Possibly a set of matched hydrogen/deuterium plasmas exists in the ASDEX dataset, which would be useful in clarifying the discrepancy between the ASDEX and TFTR results.

E. Relationship to Multi-Tokamak Scaling

For some time, power-law regression analysis has been used to determine the global scaling of τ_E with magnetic field, plasma density, plasma size, and other parameters under engineering control. Early regression analysis by Hugill and Sheffield [76] included the plasma's isotopic composition as a regression variable since the contributing tokamaks typically operated in different isotopes. They obtained a scaling relation $\tau_E^{OH} \propto \overline{n}_e{}^{.65} a^{0.6} B_T^{0.8} A_i^{0.80\pm0.25}$ from an Ohmic database from over ten tokamaks. The confidence in the deduced isotope scaling was limited in part by the fact that, with the exception of Alcator and TFR, each tokamak contributed data for either hydrogen or deuterium, but not both. Pfeiffer and Waltz[77] analyzed a somewhat larger, but overlapping, Ohmic dataset with some additional constraints, principally that more diagnostic data was required for each discharge, and that discharges with hollow density or temperature profiles were excluded. Their best-fit was $\tau_{Ee} \propto \overline{n}_e{}^{0.90\pm0.08} a^{0.98\pm0.20} R^{1.63\pm0.31} Z_{eff}^{0.23\pm0.11}$, with no isotopic dependence whatsoever. The Hugill-Sheffield expression with its isotopic scaling was found to be a poor fit to the dataset collected by Pfeiffer and Waltz. However, if only R, a, $\overline{n}_e$, and A_i were considered as regression variables, then a scaling relation $\tau_{Ee} \propto \overline{n}_e{}^{0.59} (R/a)^{1.59} A_i^{0.30}$ was an acceptable fit to the Pfeiffer-Waltz dataset.

Multi-tokamak database assessments of global energy confinement scaling in L-mode plasmas have also suffered from the absence of isotope variation within the contributed individual tokamak datasets. Consequently, these studies have not attempted to infer isotope scaling by comparing τ_E in different tokamaks – which is the standard technique for inferring size scaling – but instead have relied on isotope scaling inferred from individual tokamaks. This is the preferred approach, since relative uncertainties are minimized by comparing plasmas in the same tokamak with similar wall conditions and diagnostics. Additional uncertainties arise from lack of data on the actual plasma composition when the beam and plasma ion species are not the same. The first study by Goldston[37] avoided any conclusion about isotopic dependence of τ_E, and instead focused entirely on size and current scaling: $\tau_E \propto I_p P_{tot}^{-0.5} R^{1.75} a^{-0.37}$. Subsequent work by Kaye and Goldston[78] and Kaye[79] refined the size, elongation, and density dependence of global τ_E ($\tau_E \propto \kappa^{0.28} B_T^{-0.09} I_p^{1.24} P_{tot}^{0.58} \overline{n}_e^{0.26} a^{-0.49} R^{1.65}$), but again refrained from inferring an isotope scaling.

In preparation for design of ITER, a comprehensive evaluation of global τ_E scaling was undertaken, culminating in the so-called ITER-89P L-mode scaling.[80,81] The ITER-89P expression for τ_E includes a a square-root of mass dependence in it, $\tau_E \propto \langle A \rangle^{0.5}$; hence, a common misconception is that L-mode discharges in a given device exhibit such a scaling. As pointed out in Reference 80, "[i]n the present ITER database, there is virtually no isotope variation within each tokamak, so that it cannot be determined by regression. We have assumed an isotope dependence proportional to $M^{0.5}$ on the basis of the results of the survey of isotope dependences conducted by Wagner et al.,[21] which shows an enhancement factor of ~ 1.4 for the energy confinement time for operation with deuterium compared to hydrogen." But Ref. 21 concerned only Ohmic confinement; possibly the authors were referring to the ASDEX L-mode results reported in Ref. 22.

Similarly, in a review of multi-tokamak τ_E regression scaling, Kaye *et al.*[82] observed "[t]he mass dependence [of standard L-mode scalings] was added later on to reflect the isotope effect as observed on various experiments. ... In all the scaling expressions given here, the plasma species dependence $M_{\mathrm{eff}}^{1/2}$ was incorporated *a posteriori*, since most of the expressions were developed from a database with only one effective mass .... The species dependence was assumed to be $M_{\mathrm{eff}}^{1/2}$, based on results from ASDEX,[19] DIII-D [sic: Doublet III],[9] and JFT-2M, although it should be pointed out that no isotope dependence was found in L-mode discharges in JET[29] and DIII-D.[70] Clearly, the mass dependence of confiement is still not well understood." Isotopic scaling in JFT-2M reported by Suzuki *et al.*[32] was cited by Kaye in support of appending the Kaye-Goldston expression with an additional $A^{0.5}$ scaling. However, the basis for this support is not clear, since the plasmas described by Suzuki were in the H-mode regime, and showed *no* improvement in deuterium versus hydrogen plasmas.

It is striking that the canonical wisdom of $\tau_E \propto A^{0.5}$ in L-mode plasmas, as expressed for example by the ITER-89P scaling expression[80] and the revised Kaye-Goldston expression,[82] exceeds the strength of the isotope effect in *all* of the tokamaks shown in Table 2 with the exception of the ECH data from DIII-D. The scaling of *thermal* energy confiement time in JET and TFTR, which is arguably the most appropriate for extrapolating energy confiement to high-density ignited plasmas which will have only a small fast-ion content, is only about half as strong, with $\tau_E^{th} \propto \langle A \rangle^{0.20}$ and $\tau_E^{th} \propto \langle A \rangle^{0.26}$ respectively.

Review of the published literature on the magnitude of the "isotope effect" does not support a hypothesis of differences between "small vs. large" machines. All prior experiments have seen a positive effect in Ohmic plasmas (except initial Alcator C results[12]); caution in such Ohmic comparisons is advised because of the dominant effects of edge conditions in such comparisons, as illustrated by our results here from TFTR and the considerable experience and analysis from ASDEX.[27] We also argue that all prior L-mode experiments have also resulted in 10% $\pm$ 10% effects on the *thermal* confiement when fast ion contributions are subtracted, (*including ASDEX*[15]). There does appear to be a much stronger "isotope effect" in enhanced confiement regimes, which are not the subject of this paper.

IV. Summary

Experiments comparing confiement in hydrogen and deuterium L-mode plasmas in TFTR are described comparing Ohmic and $D^o \rightarrow H^+$ to $D^o \rightarrow D^+$ neutral-beam-injection at powers up to 7 MW. In plasmas with well-matched density profies, we observe an $\sim$ (15 $\pm$ 5)% increase in global τ_E between hydrogen and deuterium target plasmas when the H/(H+D) ratio is changed from (10 $\pm$ 3)% to (65 $\pm$ 5)%. Approximately half of this increase can be attributed to differences in beam stored energy; there remains a modest but reproducible improvement in thermal τ_E. Higher T_e was realized in the deuterium discharges, primarily in the core ($r/a < 0.3$). The clearest effect on local transport was an improvement in core χ_e. We discern no appreciable isotope effect on local χ_i, χ_ϕ, particle transport, Z_{eff}, or sawtooth frequency or re-heat. These L-mode transport results are in good agreement with JET, which implies a scaling of thermal τ_E proportional to mass to the 0.26 power, that is about one-half the strength of the effect used in ITER-89P.

References

[1] F. Romanelli, Plasma Phys. Controlled Fusion **31**, 1535 (1989).

[2] F. W. Perkins, Issues in tokamak/stellarator transport and confiement enhancement mechanisms, Technical Report PPPL-2708, Princeton Plasma Physics Laboratory, 1990.

[3] B. Coppi, The isotopic effect on plasma confiement, in *Plasma Physics and Controlled Nuclear Fusion Research, 1990*, volume 2, page 413, IAEA, Vienna, 1991, (Washington Conference).

[4] T. T. Group, Decharges a fort courant dans TFR, in *Plasma Physics and Controlled Nuclear Fusion Research, 1974*, volume 1, pages 135–145, IAEA, Vienna, 1975, (Tokyo conference).

[5] B. Coppi, G. Lampis, F. Pegoraro, L. Peroni, and S. Segre, High temperature regimes in magnetically confied plasmas in the Alcator tokamkak, Technical Report PRR-7524, Massachusetts Institute of Technology, 1975.

[6] M. Murakami et al., Phys. Rev. Lett. **42**, 655 (1979).

[7] D. Meade et al., PDX experimental results, in *Plasma Physics and Controlled Nuclear Fusion Research, 1980*, volume 1, pages 665–677, IAEA, Vienna, 1981, (Brussels Conference).

[8] S. Ejima et al., Nucl. Fusion **22**, 1627 (1982).

[9] J. C. DeBoo et al., Nucl. Fusion **26**, 211 (1986).

[10] M. Abe et al., Nucl. Fusion **29**, 1659 (1989).

[11] E. S. Marmar, J. E. Rice, J. L. Terry, and F. H. Seguin, Nucl. Fusion **22**, 1567 (1982).

[12]B. Blackwell et al., Energy and impurity transport in the Alcator C tokamak, in *Plasma Physics and Controlled Nuclear Fusion Research, 1982*, volume II, page 27, IAEA, Vienna, 1983, (Baltimore Conference).

[13]A. G. Barsukov et al., Investigation of plasma confiement and injection heating in the T-11 tokamak, in *Plasma Physics and Controlled Nuclear Fusion Research, 1982*, volume I, page 83, IAEA, Vienna, 1983, (Baltimore Conference).

[14]F. Wagner et al., Confiement and β_p-studies in neutral-beam-heated ASDEX plasmas, in *Plasma Physics and Controlled Nuclear Fusion Research, 1982*, volume I, page 43, IAEA, Vienna, 1983, (Baltimore Conference).

[15]A. Stäbler et al., Energy confiement scaling of ASDEX L- and H-discharges, in *Heating in Toroidal Plasmas*, page 3, CEC, Rome, 1984.

[16]F. Wagner, Nucl. Fusion **25**, 525 (1985).

[17]H. Niedermeyer et al., Achievement of regimes with high density, low q_a, and good confiement on ASDEX, in *Plasma Physics and Controlled Nuclear Fusion Research, 1986*, volume I, page 125, IAEA, Vienna, 1987, (London Conference).

[18]K. Steinmetz et al., Nucl. Fusion **29**, 277 (1989).

[19]H. Murmann et al., The isotope dependence of global confiement in ohmically and auxiliary heated ASDEX plasmas, in *15th European Conference on Controlled Fusion and Plasma Heating*, page 3, Dubrovnik, 1988, European Physical Society.

[20]G. Fussmann et al., Improved confiement regimes with Ohmic and with counter-injection heating in ASDEX, in *Plasma Physics and Controlled Nuclear Fusion Research, 1988*, volume I, page 145, IAEA, Vienna, 1987, (Nice Conference).

[21]F. Wagner et al., Isotope dependence of ohmic discharge parameters of Asdex, in *16th European Conference on Controlled Fusion and Plasma Heating*, volume 1, page 195, Venice, 1989, European Physical Society.

[22]F. Wagner et al., The isotope dependence of confiement in ASDEX: Part 2, in *17th European Conference on Controlled Fusion and Plasma Heating*, volume 1, page 58, Amsterdam, 1990, European Physical Society.

[23]K. McCormick et al., J. Nucl. Mater. **176 & 177**, 89 (1990).

[24]M. Bessenrodt-Weberpals et al., J. Nucl. Mater. **176 & 177**, 538 (1990).

[25]M. Bessenrodt-Weberpals et al., Nucl. Fusion **31**, 155 (1991).

[26]A. Kallenbach et al., Plasma Phys. Controlled Fusion **33**, 595 (1991).

[27]M. Bessenrodt-Weberpals et al., Nucl. Fusion **33**, 1205 (1993).

[28]J. G. Cordey et al., Particle and energy confiement in ohmically heated JET plasmas, in *Plasma Physics and Controlled Nuclear Fusion Research, 1984*, volume 1, pages 167–179, Vienna, 1985, IAEA, (London Conference).

[29]J. G. Cordey et al., Energy confiement in JET with ohmic heating and strong auxiliary heating, in *Plasma Physics and Controlled Nuclear Fusion Research, 1986*, volume I, page 99, IAEA, Vienna, 1987, (Kyoto Conference).

[30]D. V. Bartlett et al., Nucl. Fusion **28**, 73 (1988).

[31]F. Tibone et al., Nucl. Fusion **33**, 1319 (1993).

[32]N. Suzuki et al., Characteristics of the H-mode in divertor configuration on JFT-2M tokamak, in *14th European Conference on Controlled Fusion and Plasma Heating*, page 217, Madrid, 1987, European Physical Society.

[33]U. Samm et al., Isotopic effects on plasma edge properties, in *16th European Conference on Controlled Fusion and Plasma Heating*, volume 3, page 995, Venice, 1989, European Physical Society.

[34]F. Alladio et al., Analysis of saturated Ohmic confiement in the Frascati Tokamak, in *Plasma Physics and Controlled Nuclear Fusion Research, 1990*, volume 1, page 153, IAEA, Vienna, 1991, (Washington Conference).

[35]H. F. Dylla et al., J. Nucl. Mater. **176 & 177**, 337 (1990).

[36]H. Dylla et al., Nucl. Fusion **27**, 1221 (1987).

[37]R. J. Goldston, Plasma Phys. Controlled Fusion **26**, 87 (1984).

[38]S. D. Scott et al., Phys. Fluids B **2**, 1300 (1990).

[39]L. R. Grisham et al., Phys. Rev. Lett. **67**, 66 (1991).

[40]H. H. Towner et al., Rev. Sci. Instrum. **63**, 4753 (1992), (Proceedings of the 9th Topical Conference on High Temperature Plasma Diagnostics, Santa Fe).

[41]J. A. Murphy, S. D. Scott, and H. H. Towner, Rev. Sci. Instrum. **63**, 4750 (1992), (Proceedings of the 9th Topical Conference on High Temperature Plasma Diagnostics, Santa Fe).

[42]D. K. Mansfield et al., Appl. Opt. **26**, 4469 (1987).

[43]J. A. Murphy, S. D. Scott, and H. H. Towner, The SNAP user's guide, Technical Report PPPL-TM-393, Princeton Plasma Physics Laboratory, 1992.

[44]D. Johnson et al., Rev. Sci. Instrum. **56**, 1015 (1985).

[45]G. Taylor et al., Rev. Sci. Instrum. **55**, 1739 (1984).

[46]F. J. Stauffer, D. A. Boyd, R. C. Cutler, and M. P. McCarthy, Rev. Sci. Instrum. **56**, 925 (1985).

[47]F. J. Stauffer et al., Rev. Sci. Instrum. **59**, 2139 (1988).

[48]A. T. Ramsey and S. L. Turner, Rev. Sci. Instrum. **58**, 1211 (1987).

[49]K. W. Hill et al., Rev. Sci. Instrum. **56**, 840 (1985).

[50]D. B. Heifetz et al., J. Vac. Sci. Technol. A **6**, 2564 (1988).

[51]R. J. Fonck et al., Phys. Rev. Lett. **63**, 520 (1989).

[52]R. J. Fonck, D. S. Darrow, and K. P. Jaehnig, Phys. Rev. A **29**, 3288 (1984).

[53]H. K. Park et al., Nucl. Fusion **32**, 1042 (1992).

[54]W. W. Heidbrink et al., Phys. Fluids B **3**, 3167 (1991), Preprint in PPPL-2777.

[55]R. Hawryluk, unknown title, in *Physics of Plasmas Close to Thermonuclear Conditions*, volume 1, page 19, CEC, Brussels, 1980.

[56]S. Tamor, Jrnl. Computational Physics **40**, 104 (1981).

[57]M. C. Zarnstorff et al., Phys. Fluids B **2**, 1852 (1990).

[58]M. C. Zarnstorff et al., Phys. Rev. Lett. **60**, 1306 (1988).

[59]M. C. Zarnstorff et al., Overview of recent TFTR results, in *Plasma Physics and Controlled Nuclear Fusion Research, 1992*, IAEA, Vienna, 1993, (Würzburg Conference).

[60]J. H. Kamperschroer et al., Rev. Sci. Instrum. **60**, 3377 (1989).

[61]S. Scott et al., Phys. Rev. Lett. **64**, 531 (1990).

[62]C. W. Barnes et al., Rev. Sci. Instrum. **61**, 3151 (1990).

[63]R. V. Budny and The TFTR group, J. Nucl. Mater. **176 & 177**, 427 (1990).

[64]R. V. Budny et al., Nucl. Fusion **32**, 429 (1992).

[65]F. X. Söldner et al., Phys. Rev. Lett. **61**, 1105 (1988).

[66]C. S. Pitcher et al., Nucl. Fusion **32**, 239 (1992).

[67]F. Wagner and U. Stroth, Plasma Phys. Controlled Fusion **35**, 1321 (1993).

[68]O. Gruber et al., Plasma Phys. Controlled Fusion **30** (1988).

[69]R. Stambaugh et al., Plasma Phys. Controlled Fusion **30**, 1585 (1988).

[70]D. P. Schissel et al., Nucl. Fusion **29**, 185 (1989).

[71]K. H. Burrell et al., Plasma Phys. Controlled Fusion **31**, 1649 (1989).

[72]R. R. Dominguez, Nucl. Fusion **31**, 2063 (1991).

[73]B. Scott, Self-consistent models of drift wave turbulence: Implications for transport scenarios, in *Plasma Physics and Controlled Nuclear Fusion Research, 1992*, volume 1, page 203, IAEA, Vienna, 1993, (Würzburg Conference).

[74]O. Gehre, K. W. Gentle, and ASDEX- and NI-team, Isotope dependence of electron particle transport in ASDEX, in *18th European Conference on Controlled Fusion and Plasma Heating*, page 97, Berlin, 1991, European Physical Society, Volume I (Berlin Conference).

[75]T. Dudok de Wit, B. P. Duval, B. Joye, and J. B. Lister, Nucl. Fusion **31**, 359 (1991).

[76]J. Hugill and J. Sheffield, Nucl. Fusion **18**, 15 (1978).

[77]W. Pfeiffer and R. E. Waltz, Nucl. Fusion **19**, 51 (1979).

[78]S. M. Kaye and R. J. Goldston, Nucl. Fusion **25**, 65 (1985).

[79]S. M. Kaye, Phys. Fluids B **28**, 2327 (1985).

[80]P. N. Yushmanov et al., Nucl. Fusion **30**, 1999 (1990), (ITER-89P).

[81]N. A. Uckan et al., Energy and particle confiement in ITER, in *Plasma Physics and Controlled Nuclear Fusion Research, 1990*, volume 3, page 307, IAEA, Vienna, 1991, (Washington Conference).

[82]S. M. Kaye et al., Phys. Fluids B **2**, 2926 (1990), Special Section: Anomalous Transport in Tokamaks: U. S. Department of Energy Transport Task Force Reviews.

[83]B. W. Stallard et al., Nucl. Fusion **30**, 2235 (1990).

[84]V. Arunasalam et al., Recent results from the PLT tokamak, in *Proceedings of the Eighth European Conference on Controlled Fusion and Plasma Physics (Prague,*

Czechoslovakia, 1977), volume 2, pages 17–28, Instutute of Plasma Physics, Czechoslovak Academy of Sciences, Prague, 1977.

[85]S. Fairfax et al., Energy and particle confiement in the Alcator tokamaks, in *Plasma Physics and Controlled Nuclear Fusion Research, 1980*, volume I, page 439, IAEA, Vienna, 1981, (Brussels Conference).

[86]M. Greenwald et al., Confiement of ohmic and ICRF heated plasmas in Alcator C-Mod, paper IAEA-CN-60/A2/4-P-2 presented at the Fifthteenth International Conference on Plasma Physics and Controlled Nuclear Fusion Research (Seville, Spain, 1994).

[87]H. W. Hendel et al., Rev. Sci. Instrum. **61**, 1900 (1990).

Condition								Energy (kJ)								
a	I_p	P_b	T_{eo} (keV)		U_{eo} (kJ/m^3)			W_e			W_i		W_b		W_{tot}^{kin}	
(m)	(kA)	(MW)	H	D	H	D		H	D		H	D	H	D	H	D
0.8	1.4	2.5	3.10	3.49	29.6	33.4	(+13%)	247	272	(+10%)	222	222	65	78	537	574
		4.6	3.42	4.39	34.3	42.6	(+24%)	275	309	(+12%)	252	256	112	159	652	730
		6.8	4.30	4.78	49.8	56.3	(+13%)	337	360	(+7%)	295	319	155	208	800	896
	0.7	4.6	2.77	3.57	19.2	23.2	(+21%)	127	150	(+18%)	116	117	97	153	343	422
		6.8	3.03	3.97	24.9	28.9	(+20%)	155	177	(+14%)	140	154	133	209	431	544
0.5	0.7	2.2	1.81	2.16	26.3	32.8	(+25%)	88	103	(+17%)	109	91	19	24	218	220
		4.6	2.63	3.48	32.2	43.4	(+35%)	93	116	(+25%)	107	102	60	76	261	298

Table 1: Kinetic measurements of central and volume-integrated stored energy for discharges of paired density profile shown in Fig. 6. Values in parentheses indicate change from H to D plasmas.

Tokamak	Matched conditions	m; $[\tau_E \propto \langle A \rangle^m]$ total	thermal	Reference
ASDEX	Y	0.34 ± 0.02		Bessenrodt,Wagner[22,27]
DOUBLET	N	0.40 ± 0.08		DeBoo[9]
DIII-D	Y	~ 0		Schissel[70]
DIII-D (ECH)	Y	~ 0.74		Stallard[83]
JET	Y	0.32 ± 0.06	0.20 ± 0.12	Tibone[31]
TFTR	Y	0.41 ± 0.12	0.26 ± 0.11	

Table 2: Review of isotope scaling in L-mode plasmas. The exponents for Doublet, DIII-D, and JET were determined from published ratios of τ_E assuming pure hydrogen and pure deuterium plasmas.

Tokamak	R (m)	a (m)	B_T (T)	I_p (MA)	$\overline{n}_{e19}$ (m^{-3})	$\tau_E^{OH}(D)/\tau_E^{OH}(H)$	Regime	Reference
TFR	0.98	0.20	5.0	0.3	4	1.45		TFR Group[4] (197
Alcator	0.54	0.10	—	—	—	—	—	Coppi[5] (1975)
PLT	1.34	0.40	3.0-3.5?	0.4-0.5?	5	1.0†	LOC	Arunasalam[84] (1
ISX-A	0.92	0.26	0.8-1.5	0.09-0.12	0.8-3.0	1.20-1.65	LOC	Murakami[6] (197
					3.0-5.0	1.3-1.5	SOC	
Alcator C	0.64	0.17	6	0.4-0.5	22	1.0	LOC	Fairfax[85] (1980)
					25-37	0.80-1.0	SOC	Fairfax[85] (1980)
PDX	1.43	0.38	1.7	0.3	2.3-4	1.2-1.8		Meade[7] (1980)
					3.0-4.0	1.8-3.2†		
ASDEX	1.65	0.40	1.9-2.4	0.15-0.44	0.8-2.5	1.20-1.27 (C)	LOC	Wagner[21,27] (198
					2.5-5.5	1.38-1.44 (C)	SOC	
			1.8-2.8	0.20-0.45	2.5-5.5	1.57 (B)	SOC	Wagner[22,27] (199
DIII	1.43	0.44	2.0-2.4	0.47	1.7-3.2	1.2-1.4	LOC	Ejima[8] (1982)
					4.3	1.45	SOC	
T11	0.70	0.20	0.9	0.11	1.5-2.5	1.4-1.5		Barsukov[13] (198
JET	3.0	1.1	1.3-3.4	1.2-3.5	0.7-3.0	1.1-1.4		Cordey[28] (1985)
	3.1	0.8-1.23	1.7-3.4	1.0-4.0	0.5-3.6	1.4-1.5		Bartlett[30] (1988)
	2.5-3.4	1.1	2.9	3.1	1.1-2.5	1.2-1.3	SOC	Tibone[31] (1993)
JFT-2M	1.3	0.27	1.2	0.1-0.3	?	1.3-1.6		Suzuki[32] (1987)
Frascati	0.83	0.23	6	0.4-0.6?	$\leq$6	$\sim$1	LOC	Alladio[34] (1990)
					12-24	1.2-1.7	SOC	
Alcator C-Mod	0.65-0.70	0.20-0.24	3.5-5.4	0.35-1.05	3-7	1.35-1.50		Greenwald[86] (19
TFTR	2.45	0.80	4.0	1.4	1.1–1.9	1.0	LOC	
					1.9–4.4	1.1	SOC	

Table 3: Review of isotope scaling in Ohmic plamas. LOC = linear Ohmic regime, SOC = saturated Ohmic regime. † denotes the ratio of τ_E in helium versus hydrogen plasmas. (B) denotes boronized walls; (C) denotes carbonized walls.

Figures

FIG. 1. Neutral beam power in MW (black solid line), diamagnetic stored energy in 0.1 MJ (red long dashed line), line-averaged density in 10^{19} m^{-3} (green short dashed line), and central toroidal rotation velocity in 10^5 m/sec (blue dot-dashed line) for two discharges. (a) $D^o \rightarrow D^+$ discharge. (b) $D^o \rightarrow H^+$ discharge. The vertical shaded region for each discharge represents the time averaging interval of the SNAP time-independent transport analysis.

FIG. 2. Total electron stored energy vs total input heating power (neutral beam plus Ohmic). Each point represents a separate analysis using the SNAP code. (a) The black triangles use TS (Thomson) with Slice & Stack; (b) The red squares use YS (radiometer) with inboard mapping; and (c) the green circles use YM (Michelson) with Partial Slice & Stack. The open symbols are for $D^o \rightarrow D^+$ and the closed symbols are for $D^o \rightarrow H^+$. The discharges below the dashed line are 0.7 MA, while those above are 1.4 MA, all for $\boldsymbol{R} = 2.45$ m.

FIG. 3. Total stored energy vs total input heating power. The red circles are large plasmas at both 1.4 MA and 0.7 MA, while the green squares are small plasmas at 0.7 MA. The open symbols are deuterium and the closed hydrogen. The error bars are on the two "paired" discharges of Fig. 1, and show the one-sigma relative uncertainty in the results. (a) electrons. The analysis of these data using second harmonic ECE emission are slightly different from Fig 2(c) because of improved ion temperature data and assumptions about neutral content. (b) ions. (c) total perpindicular energy from magnetics. The low and high current data are not clearly separated here because of the large contribution from beam stored energy at low density and current.

FIG. 4. Comparisons of calculated and measured diamagnetic stored energy and neutrons. (a) Calculated ("kinetic") stored energy versus measured (from magnetics). The symbols differentiate deuterium and hydrogen and large vs small plasmas. The data is consistent with unity slope, but with a 65 kJ

negative offset of the measured diamagnetism. (b) Calculated DD neutron source strength vs the measurement from the fission chamber system.[87] The data is consistent with being proportional, but at 80–90% of the measured value. (c) Ratio of calculated-to-measured neutron source strength vs ratio of calculated-to-measured diamagnetic stored energy. The measured stored energy has been increased by 65 kJ for all this data. The error bars are again on the two "paired" discharges of Fig. 1, and show the one-sigma relative uncertainty in the results.

FIG. 5. Electron particle source rate from wall recycling, estimated to be proportional to the measured $\boldsymbol{H}_\alpha$ recycling light, vs the total number of electrons in the discharge (the volume times the average electron density). The green squares are 1.4 MA large plasmas, the red triangles 0.7 MA large plasmas, and the blue circles 0.7 MA small plasmas. On each symbol is overlayed an x for a deuterium discharge and a plus for hydrogen.

FIG. 6. Plasma kinetic profiles vs major radius, comparing deuterium and hydrogen L-mode discharges of the same radius, current, beam power, and electron density profile. The red solid line is the deuterium profile, the green dashed line is hydrogen. The 3 columns are of electron density, electron temperature, and ion temperature. Each row is for a different size, current, and beam power.

FIG. 7. Integrated power flow normalized to total input power inside the radius vs minor radius, for the $D^o \rightarrow D^+$ discharge of Fig. 1 and 6(b). (a) electron channels. (b) ion channels. (c) Total input power vs minor radius, the quantity used to normalize the data in (a) and (b). Here the open circles are from the $D^o \rightarrow D^+$ discharge, and the closed circles are the hydrogen discharge to illustrate the relative matching and uncertainties.

FIG. 8. Total electron and ion thermal diffusivity, and momentum diffusivity vs minor radius, for the same two discharges of Fig. 1 and 6(b). The dark red line is deuterium and the light green line is hydrogen.

FIG. 9. Integrated energy confiement time out to the one-quarter minor radius vs input power. Open symbols are deuterium and closed are hydrogen; circles are electron confiement and triangles ion. The lines serve to guide the eye between different points of a scan; no trends with power are claimed. The error bars are expected to be larger at low power in this figure.

FIG. 10. Central momentum (velocity times mass density) vs total integrated torque. The central momentum is used to have the least susceptibility to errors in the edge rotation value. Open symbols are again deuterium, closed are hydrogen. Only 1.4 MA large plasma data are shown.

FIG. 11. Plasma parameters vs line-integrated electron density, for many different density scans during the 1989–1990 period. The large green diamonds are the hydrogen density scan, while the other symbols are various deuterium scans. All plasmas are 1.4 MA discharges at -55.7 kA TF and 2.45 m major radius. (a) loop voltage. (b) visible bremsstrahlung signal. (c) density peakedness.

FIG. 12. More plasma parameters vs line-integrated electron density, for the same scans as Figure 11. (a) diamagnetic stored energy. (b) global confiement time.

FIG. 13. Plasma parameters vs time for 1 hydrogen (green line with diamonds) and 5 deuterium discharges, including a deuterium one from this experiment (red line with circles), all with approximately (within $\pm$5%) the same line-integrated density of 4×10^{15} cm^{-2}. The hydrogen discharge (at the same 1.4 MA plasma current) generally has higher loop voltage and Ohmic heating, lower Z_{eff} and stored energy and confiement time. (a) plasma current. (b) loop voltage. (c) Ohmic heating power. (d) visible bremsstrahlung. (e) line-integrated density at 2.47 m major radius. (f) line-integrated density at the inboard edge at 1.80 m major radius. (g) diamagnetic stored energy. (i) confiement time. All data has been smoothed in time with a 0.25 second filter.

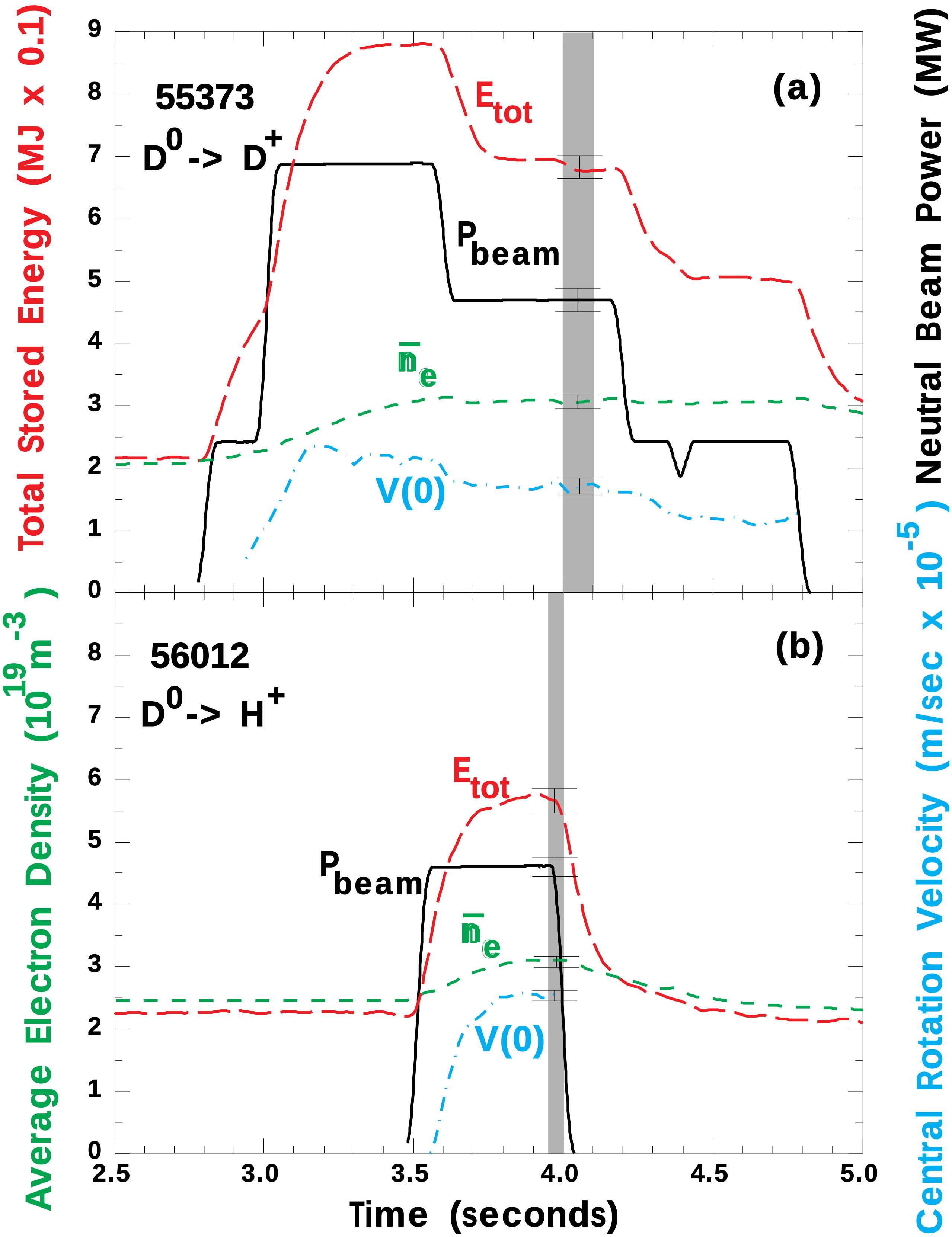

Total Stored Energy (MJ x 0.1)
Neutral Beam Power (MW)
55373
D^0 -> D^+
(a)
E_{tot}
P_{beam}
$\bar{n}_e$
V(0)
56012
D^0 -> H^+
(b)
E_{tot}
P_{beam}
$\bar{n}_e$
V(0)
Average Electron Density (10^{19} m^{-3})
Central Rotation Velocity (m/sec x 10^{-5})
Time (seconds)

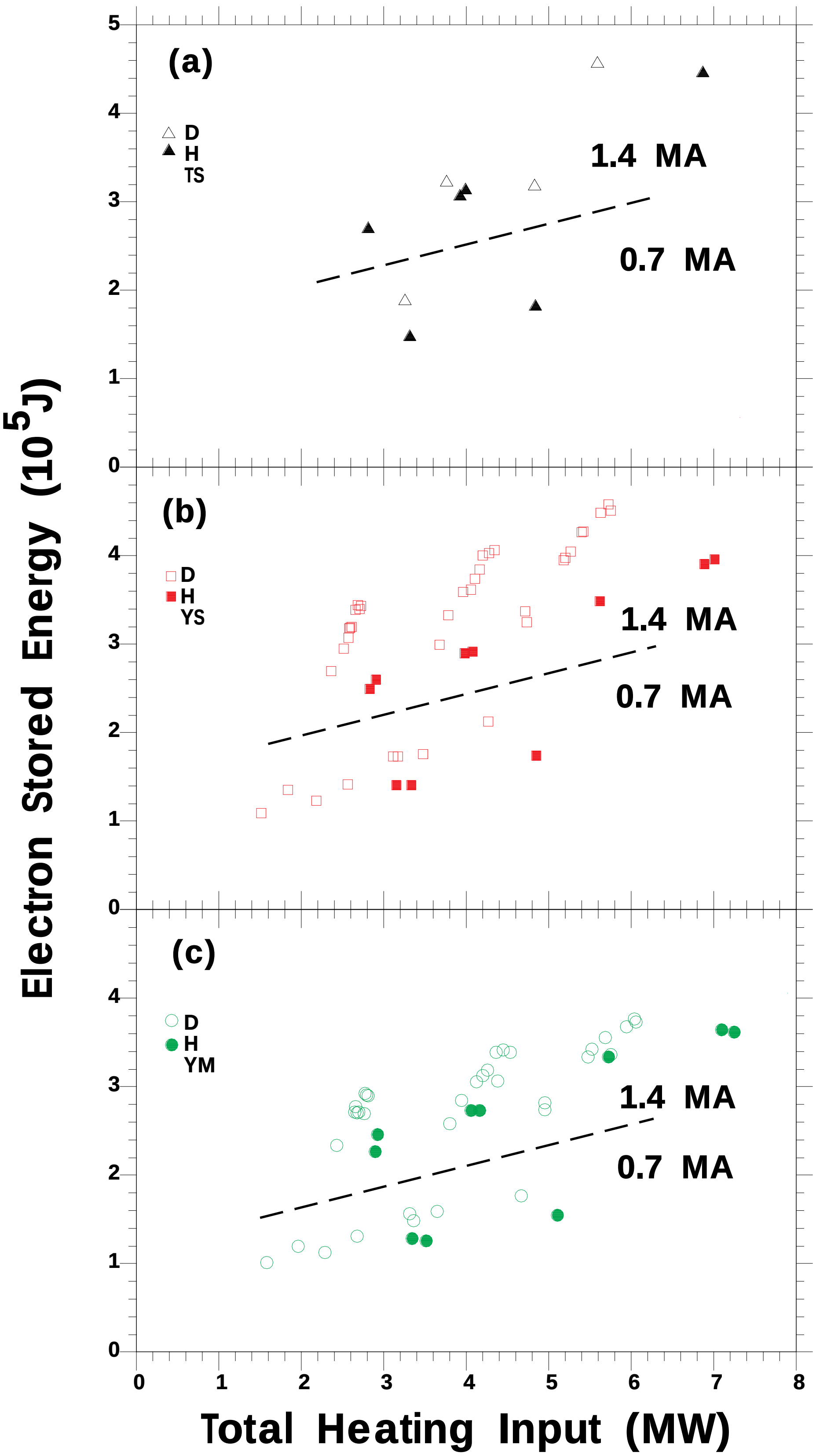

(a)
D
H
TS
1.4 MA
0.7 MA
(b)
D
H
YS
1.4 MA
0.7 MA
(c)
D
H
YM
1.4 MA
0.7 MA
Electron Stored Energy (10^5J)
Total Heating Input (MW)

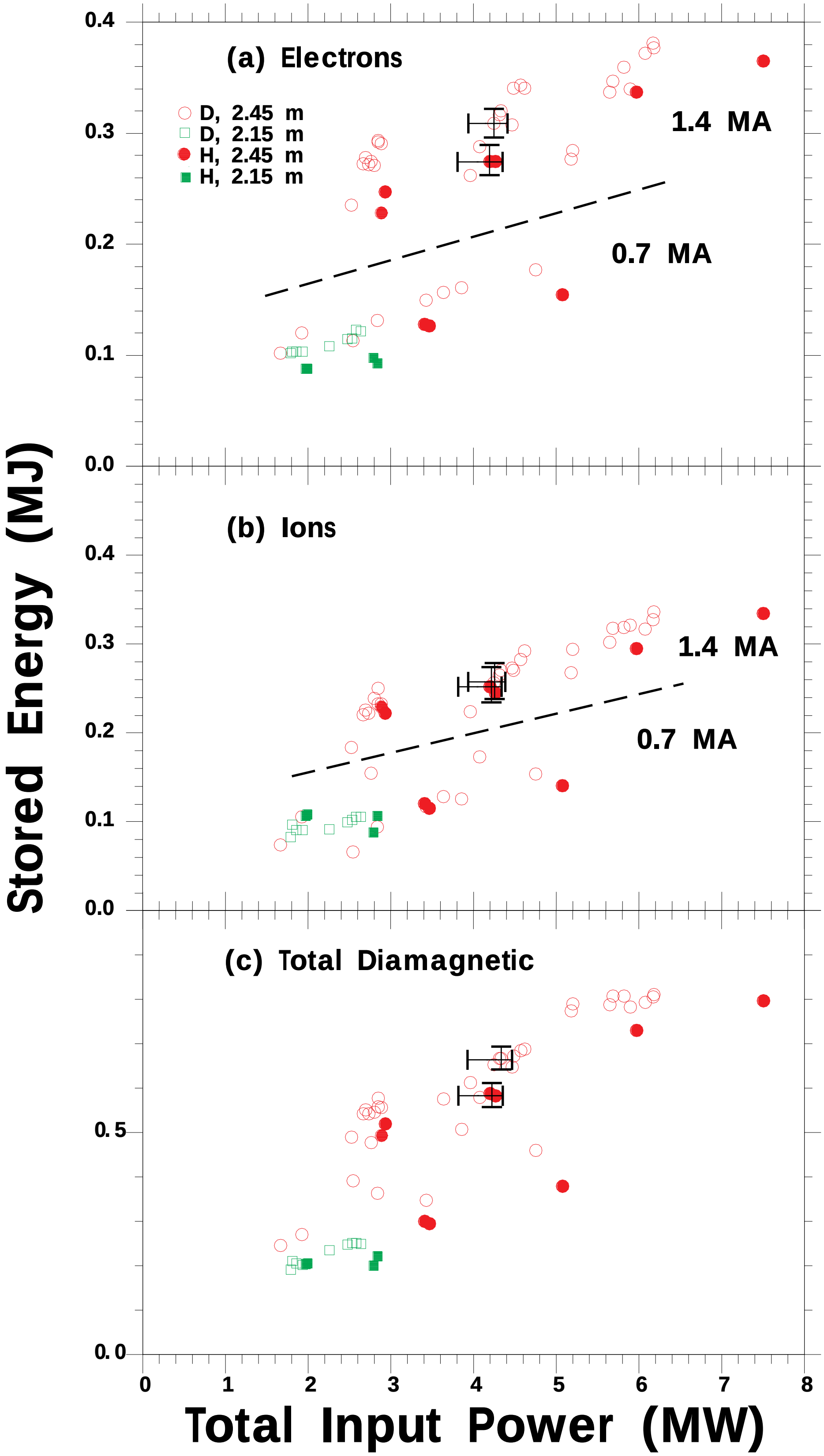

(a) Electrons
D, 2.45 m
D, 2.15 m
H, 2.45 m
H, 2.15 m
1.4 MA
0.7 MA
(b) Ions
1.4 MA
0.7 MA
(c) Total Diamagnetic
Stored Energy (MJ)
Total Input Power (MW)
0.0
0.1
0.2
0.3
0.4
0.5
0
1
2
3
4
5
6
7
8

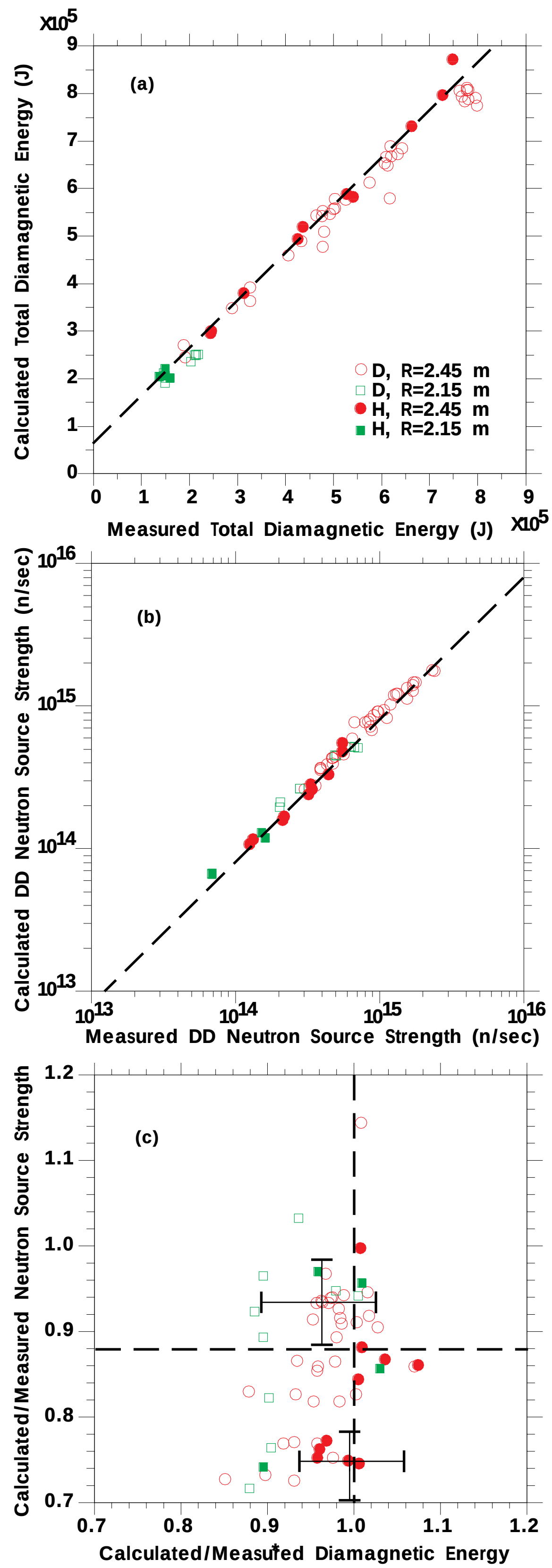

X10^5
(a)
Calculated Total Diamagnetic Energy (J)
Measured Total Diamagnetic Energy (J)
D, R=2.45 m
D, R=2.15 m
H, R=2.45 m
H, R=2.15 m
(b)
Calculated DD Neutron Source Strength (n/sec)
Measured DD Neutron Source Strength (n/sec)
(c)
Calculated/Measured Neutron Source Strength
Calculated/Measured Diamagnetic Energy

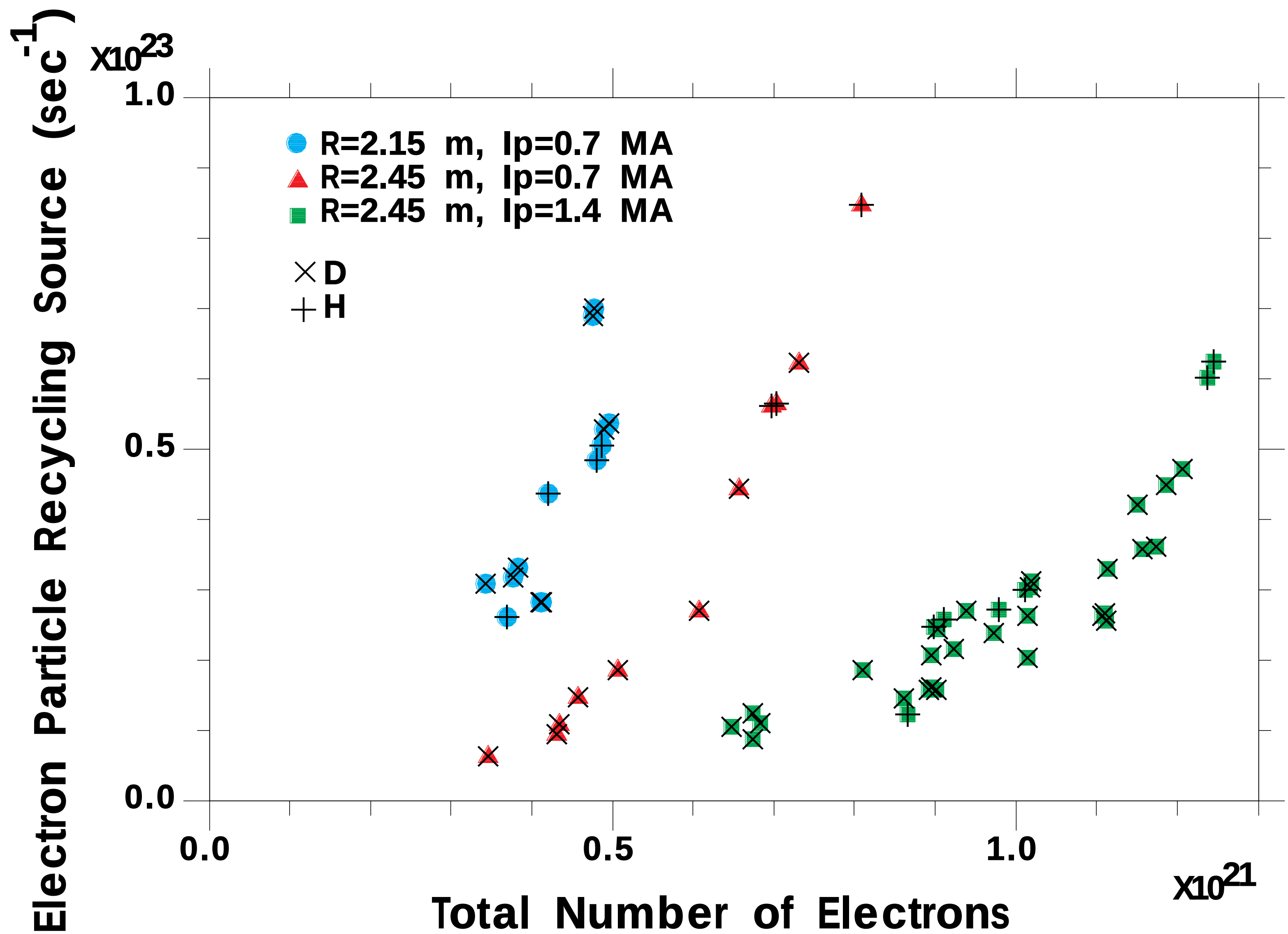

Electron Particle Recycling Source (sec^{-1})
X10^{23}
1.0
0.5
0.0
R=2.15 m, Ip=0.7 MA
R=2.45 m, Ip=0.7 MA
R=2.45 m, Ip=1.4 MA
D
H
0.0
0.5
1.0
X10^{21}
Total Number of Electrons

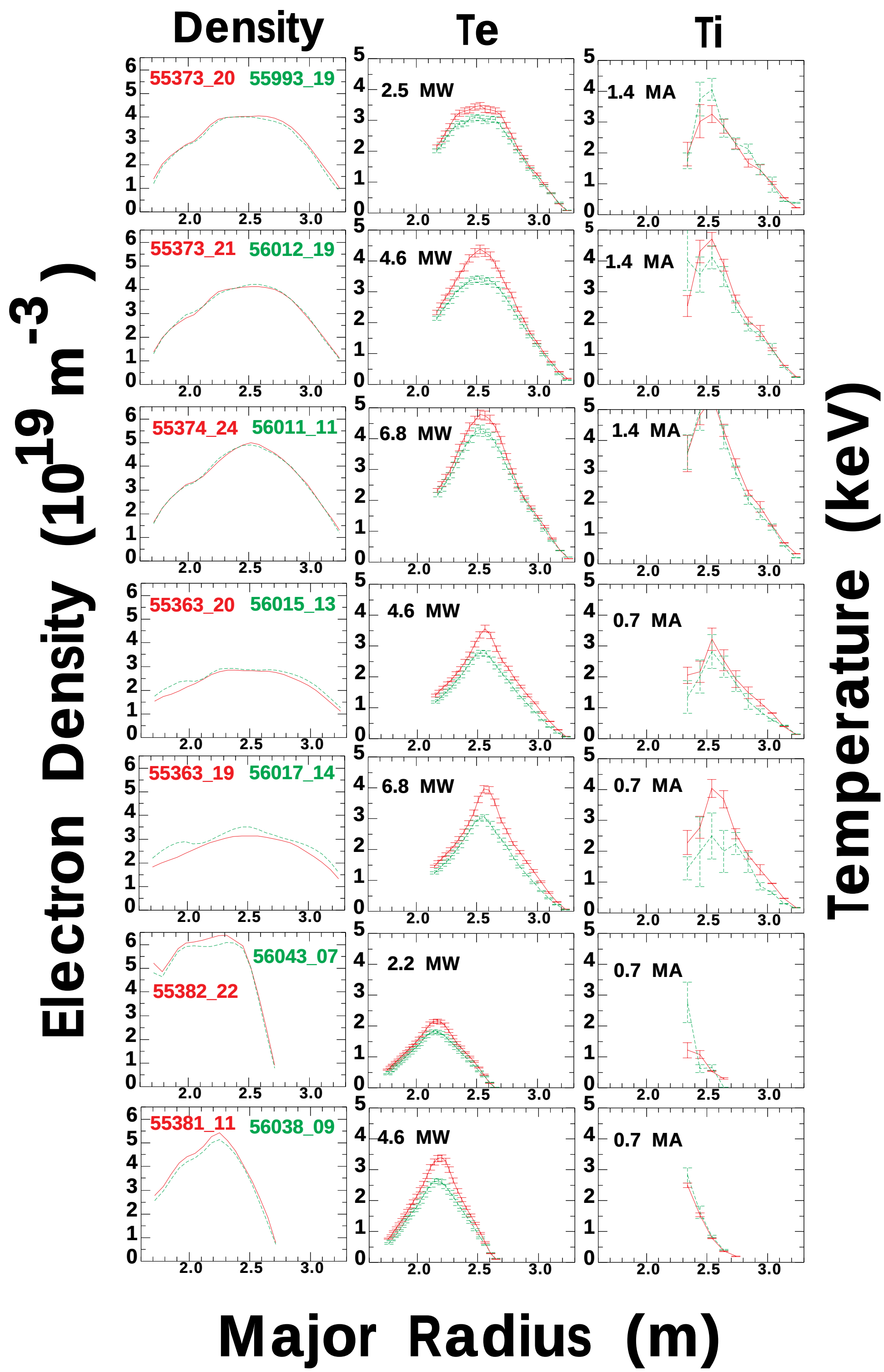

Density
Te
Ti
55373_20
55993_19
2.5 MW
1.4 MA
55373_21
56012_19
4.6 MW
1.4 MA
55374_24
56011_11
6.8 MW
1.4 MA
55363_20
56015_13
4.6 MW
0.7 MA
55363_19
56017_14
6.8 MW
0.7 MA
56043_07
55382_22
2.2 MW
0.7 MA
55381_11
56038_09
4.6 MW
0.7 MA
Electron Density (10^{19} m^{-3})
Temperature (keV)
Major Radius (m)

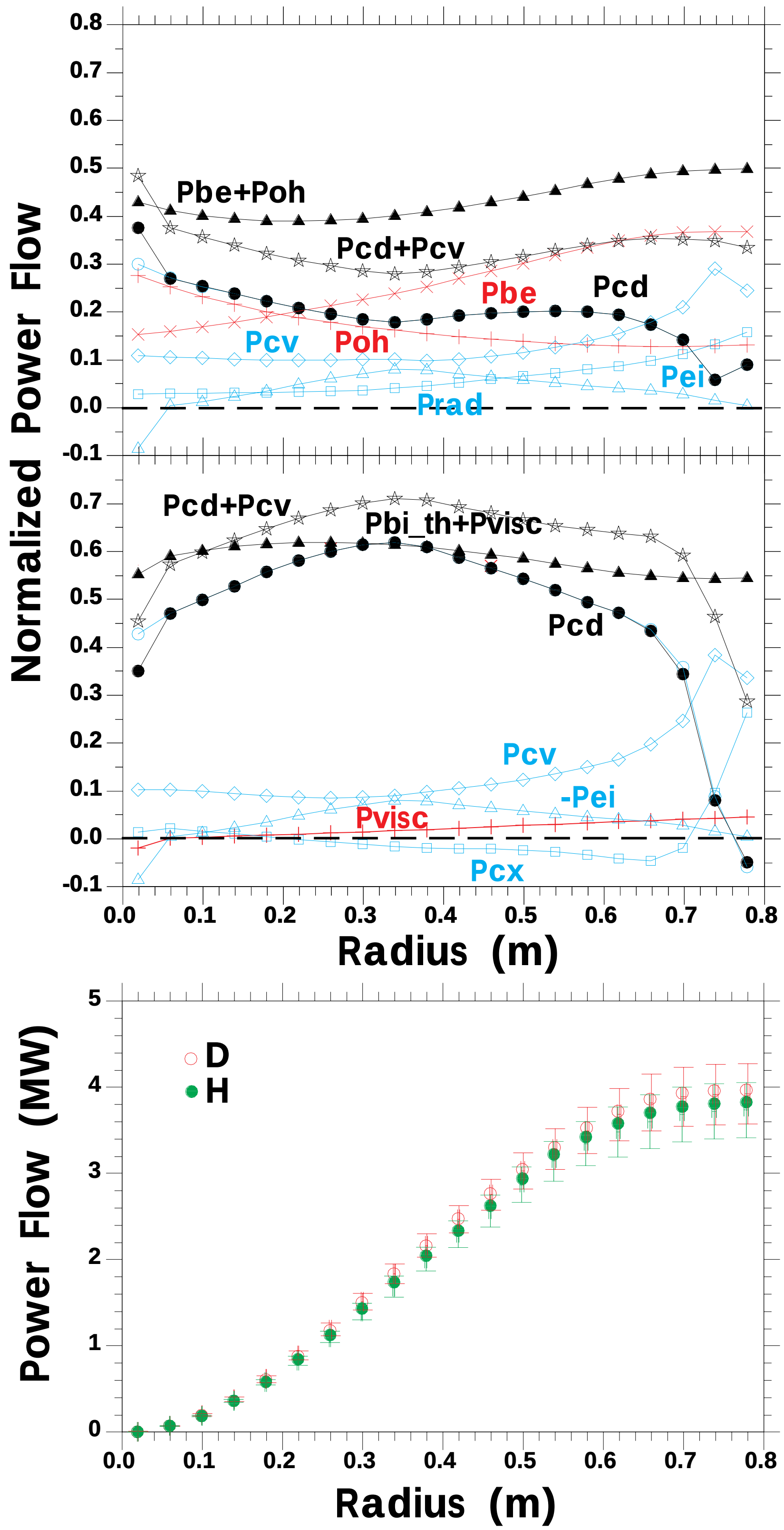
Normalized Power Flow
Pbe+Poh
Pcd+Pcv
Pbe
Pcd
Pcv
Poh
Pei
Prad
Pcd+Pcv
Pbi_th+Pvisc
Pcd
Pcv
-Pei
Pvisc
Pcx
Radius (m)
Power Flow (MW)
D
H
Radius (m)

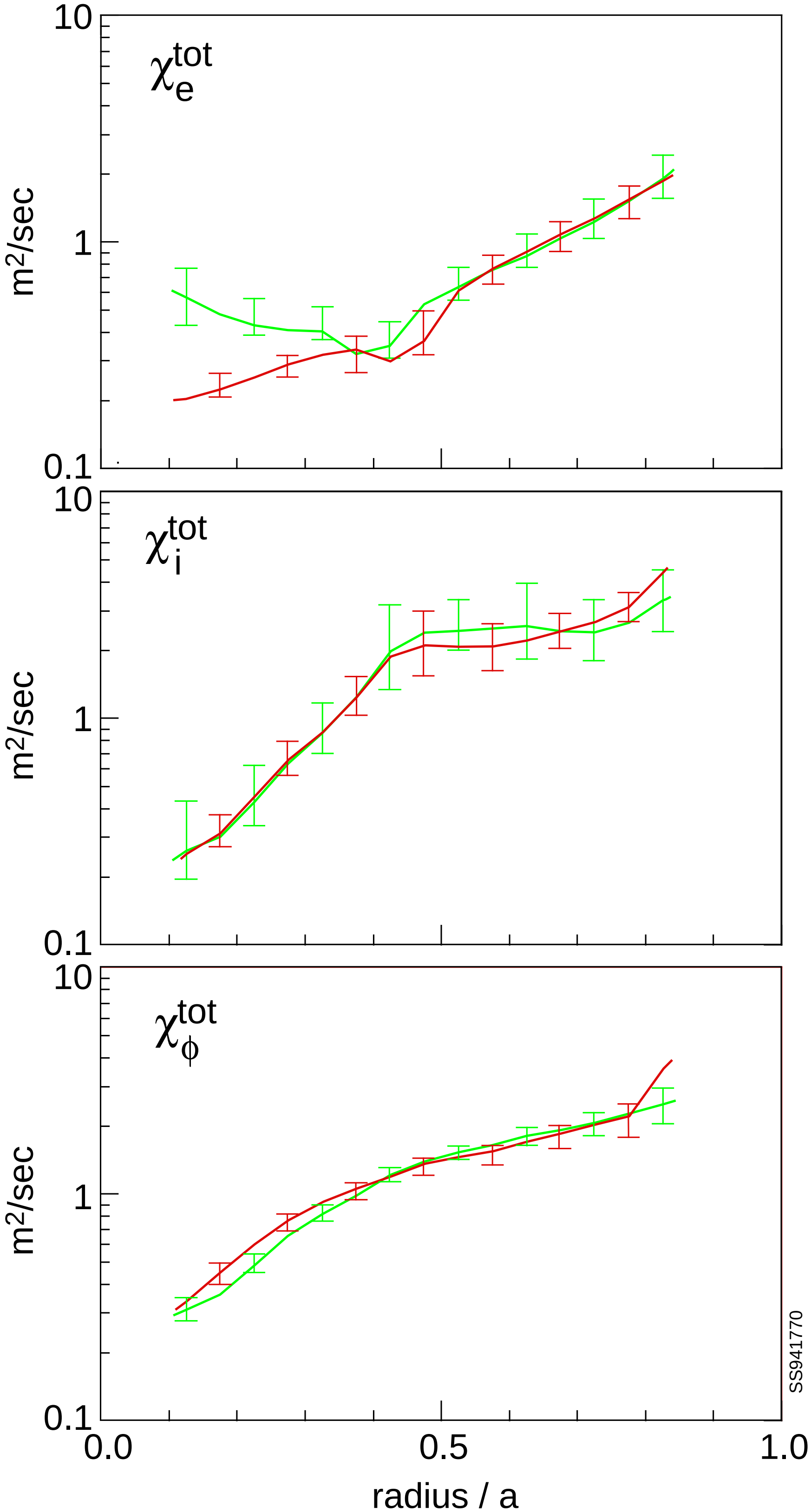
10
χ_e^{tot}
1
0.1
m²/sec
10
χ_i^{tot}
1
0.1
m²/sec
10
χ_ϕ^{tot}
1
0.1
m²/sec
SS941770
0.0
0.5
1.0
radius / a

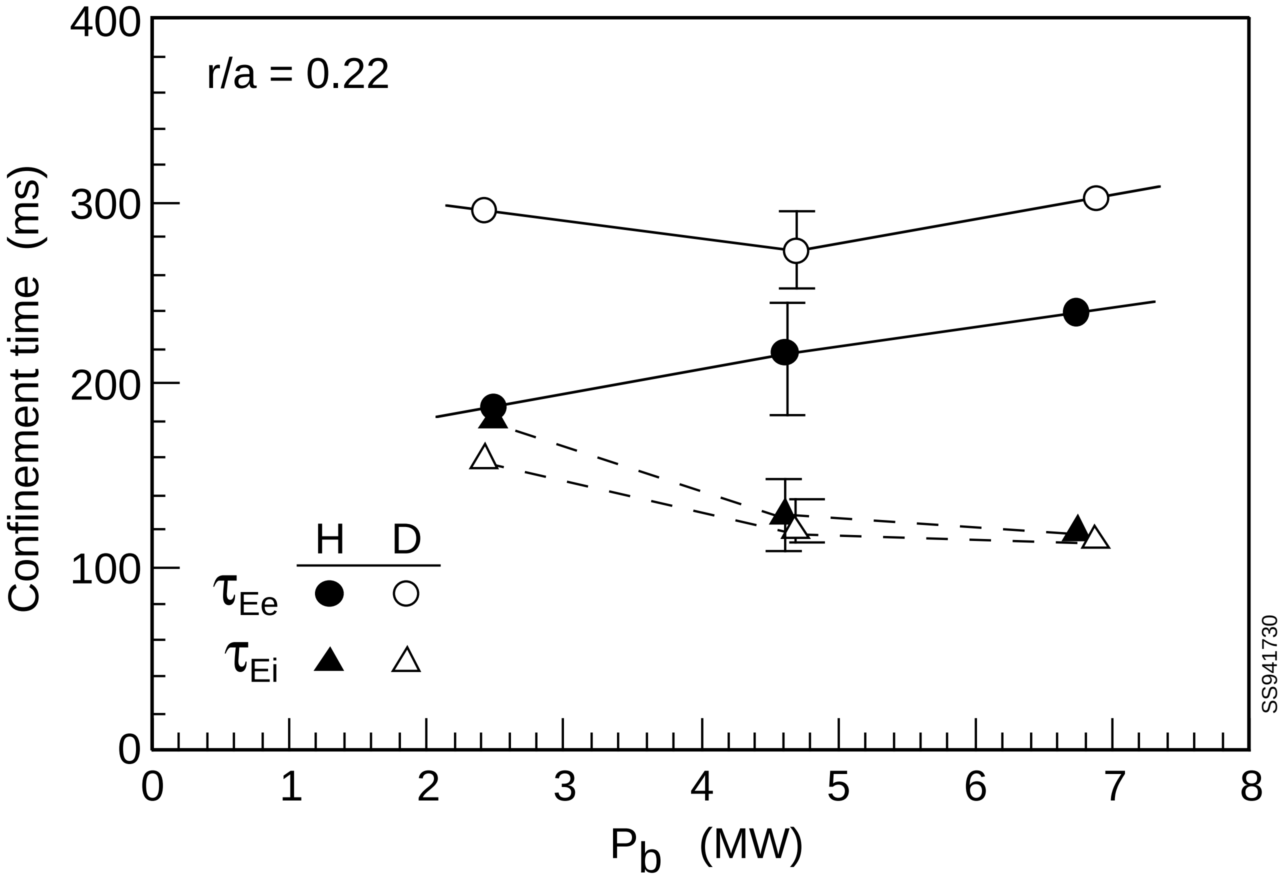

r/a = 0.22
Confinement time (ms)
400
300
200
100
0
H
D
τ_{Ee}
τ_{Ei}
0
1
2
3
4
5
6
7
8
P_b (MW)
SS941730

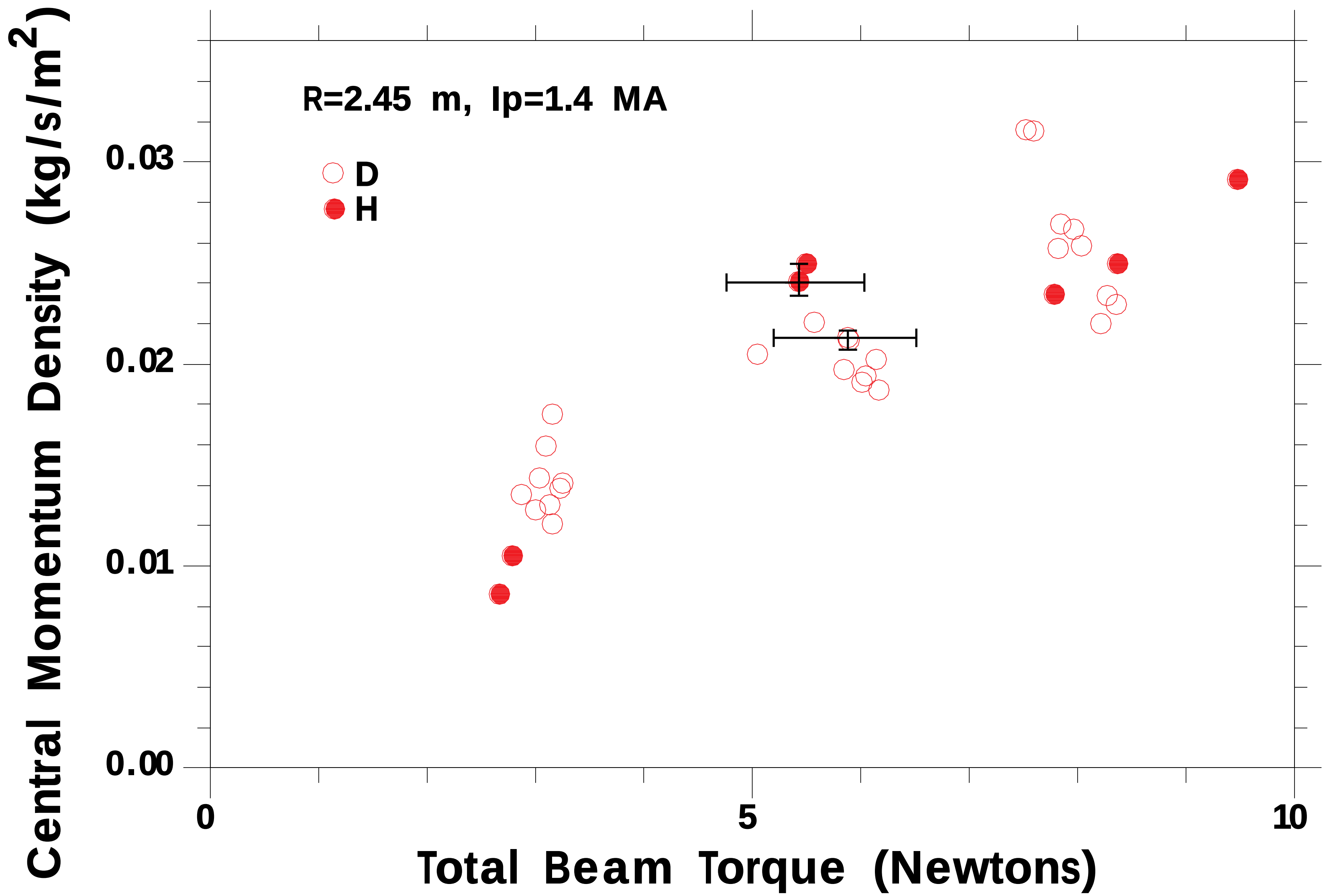

R=2.45 m, Ip=1.4 MA
D
H
0.00
0.01
0.02
0.03
0
5
10
Central Momentum Density (kg/s/m^2)
Total Beam Torque (Newtons)

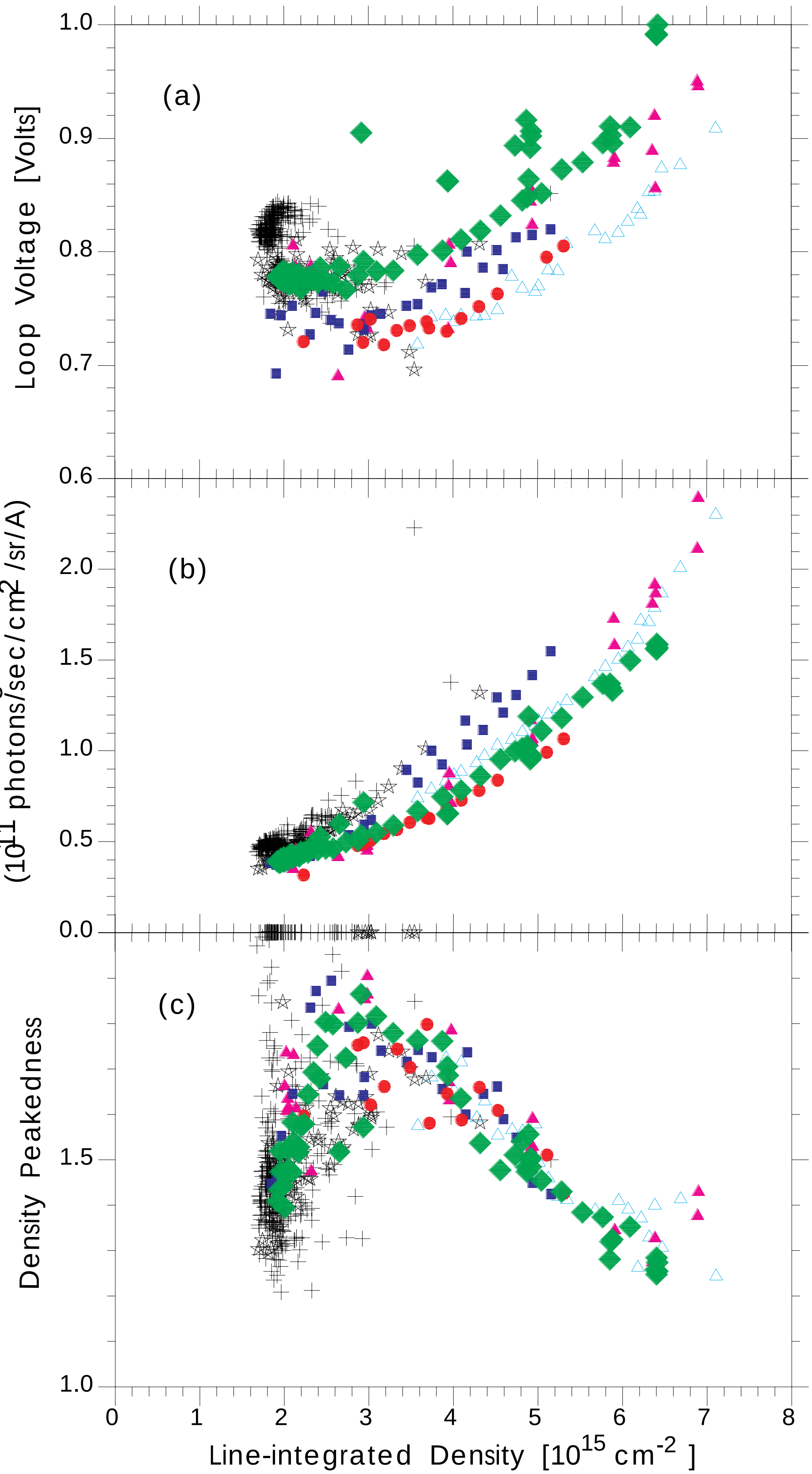

(a)
(b)
(c)
Loop Voltage [Volts]
VB Brightness (10^11 photons/sec/cm^2/sr/A)
Density Peakedness
Line-integrated Density [10^15 cm^-2]
1.0
0.9
0.8
0.7
0.6
2.0
1.5
1.0
0.5
0.0
1.5
1.0
0
1
2
3
4
5
6
7
8

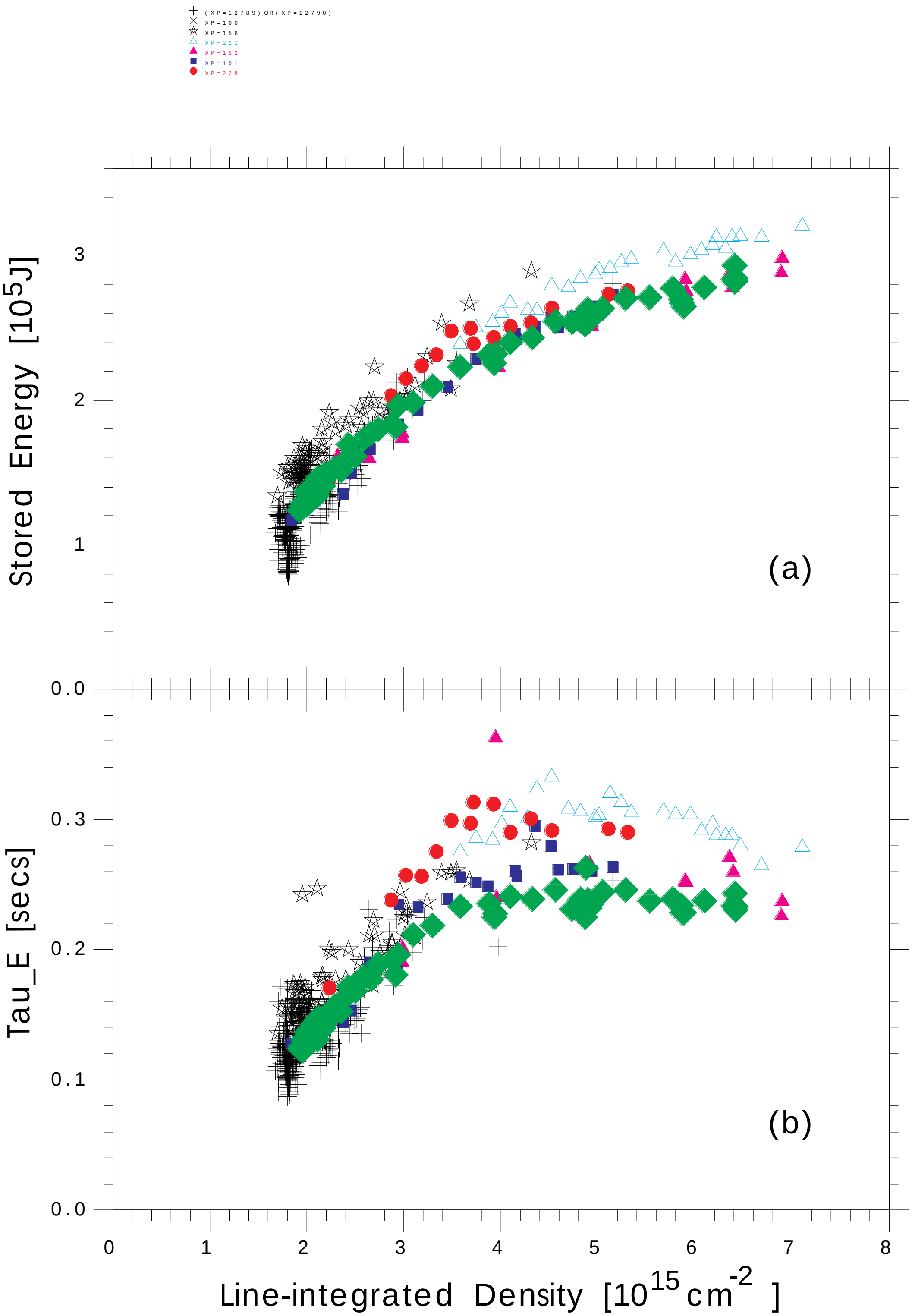

(XP=12789) OR (XP=12790)
XP=100
XP=156
XP=221
XP=152
XP=101
XP=228
Stored Energy [10^5 J]
3
2
1
0.0
(a)
Tau_E [secs]
0.3
0.2
0.1
0.0
(b)
0
1
2
3
4
5
6
7
8
Line-integrated Density [10^15 cm^-2]

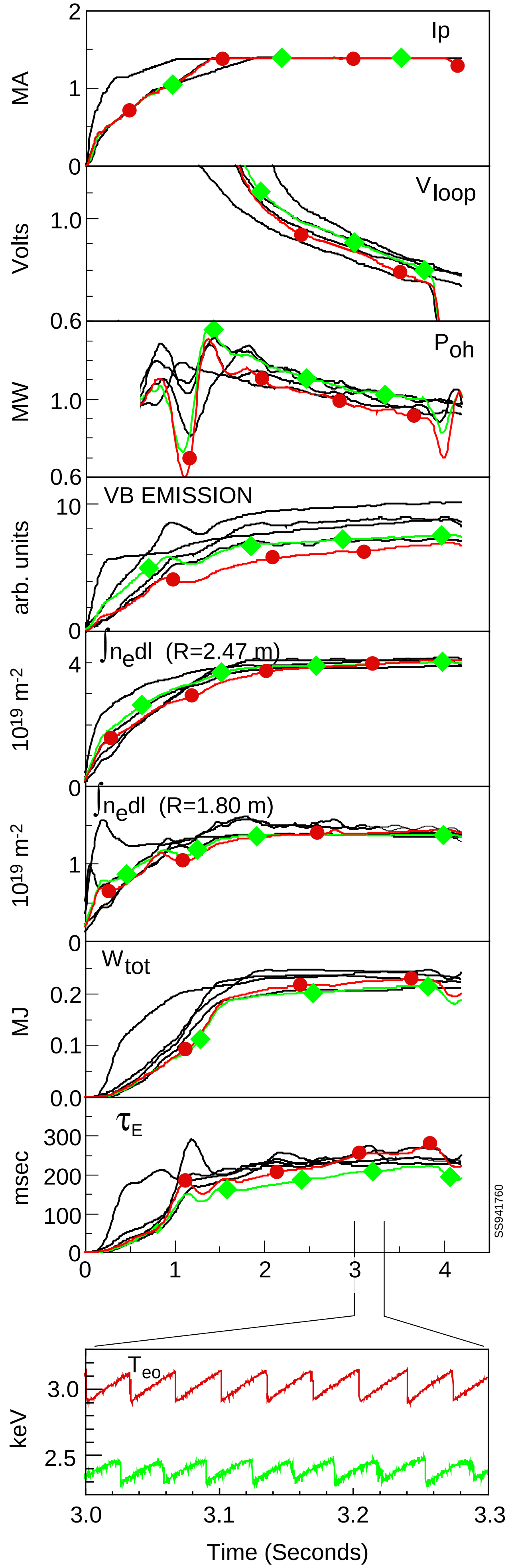

Ip
MA
Vloop
Volts
Poh
MW
VB EMISSION
arb. units
∫nedl (R=2.47 m)
10^19 m^-2
∫nedl (R=1.80 m)
10^19 m^-2
Wtot
MJ
τE
msec
SS941760
Teo
keV
Time (Seconds)